

February 11, 2019

Lower Nooksack River Geomorphic Assessment

APPENDIX D

River Processes: Hydraulics, Bed and Bank Material, Sediment Transport, and Regime Appendix

Prepared for:

Whatcom County Flood Control Zone District
322 N Commercial Street, Suite 120
Bellingham, WA 98225



WHATCOM COUNTY
Washington

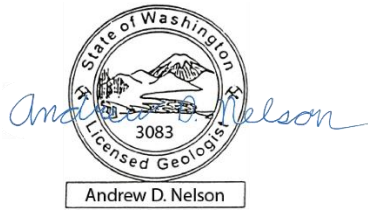
Submitted by:

**Northwest Hydraulic
Consultants**
215 W. Holly #H-21
Bellingham WA

nhc
northwest hydraulic consultants

REPORT SUBMISSION:

Northwest Hydraulic Consultants
Andrew Nelson, LG



**LOWER NOOKSACK GEOMORPHIC ASSESSMENT
RIVER PROCESSES: HYDRAULICS, BED AND BANK MATERIAL,
SEDIMENT TRANSPORT, AND REGIME APPENDIX**

FINAL REPORT

Prepared for:

Applied Geomorphology
Bozeman, Montana

On behalf of:

Whatcom County Flood Control Zone district
Bellingham, WA

Prepared by:

Northwest Hydraulic Consultants Inc.
Bellingham, WA

July 5, 2018

Prepared by or under the direct supervision of:

Andrew Nelson, M.Sc., LG
Geomorphologist
Analysis and Authorship

Dave McLean, PhD
Principal River Engineer
Reviewer

DISCLAIMER

This document has been prepared by Northwest Hydraulic Consultants Inc. in accordance with generally accepted engineering practices and is intended for the exclusive use and benefit of Applied Geomorphology and Whatcom County River and Flood and their authorized representatives for specific application to the Lower Nooksack River between Marietta and Deming, WA. The contents of this document are not to be relied upon or used, in whole or in part, by or for the benefit of others without specific written authorization from Northwest Hydraulic Consultants Inc. No other warranty, expressed or implied, is made.

Northwest Hydraulic Consultants Inc. and its officers, directors, employees, and agents assume no responsibility for the reliance upon this document or any of its contents by any parties other than Applied Geomorphology and Whatcom County River and Flood.

EXECUTIVE SUMMARY

This report describes results of NHC's observations and calculations related to hydraulic conditions, bed and bank material, sediment mobility, and regime analysis along the Lower Nooksack River in order to clarify fundamental physical processes that control the cross-section and profile geometry of the river. It supports the accompanying main report, and so focuses on direct reporting of observations, calculations, and methods applied, in the anticipation that interpretation of these results will be included in the main report for the project.

Hydraulic conditions were evaluated by extracting depth, slope, and shear stress information from the County's Full Equations (FEQ) hydraulic model of the river for floods ranging from a 2- to 100-year recurrence interval. Results were evaluated for the water surface maximum along the whole river profile and for the whole duration of flood hydrographs at select output locations. The channel bed profile is distinctly concave, and flood water surface slopes correspondingly decline in the downstream direction, dropping by an order of magnitude from a typical slope of about 0.3% in Upper Reach 4 to 0.02% in Upper Reach 1. Channel depth also generally increases in the downstream direction. During the 2-year flood, typical depths increase by a factor of two from 10-12 feet in the upstream portion of Lower Reach 4 (no current thalweg depth data are available for Upper Reach 4) to 20-25 feet in Lower Reach 2 and Upper Reach 1. Because shear stress—a measure of the channel's ability to move sediment—is a function of the channel depth and slope, increasing depth in the downstream direction partially counteracts the decrease in slope. However, the slope decreases more than depth increases, and so typical channel shear stress also decreases in the downstream direction: during a 2-year flood, it drops from greater than 100 Pa (capable of transporting medium-sized cobbles) upstream to approximately 20 Pa (capable of moving only relatively fine <45 mm gravel) through Upper Reach 1.

The grainsize distribution of channel bed material was determined by 15 pebble counts between RM 6 and 36, and 7 previously collected (NHC, 2015) bulk samples between RM 2 and 6. The grainsize distribution declines from cobble-dominant in Upper Reach 4 to sand-dominant by Middle Reach 1. Key transition zones occur in Lower Reach 4a, with a shift from cobble- to gravel-dominated bed material, and at the transition between Upper and Lower Reach 3 with an abrupt loss of any cobble-sized material and shift of the surface D_{50} from about 45 to about 32 mm. From the head of Lower Reach 3, the grainsize gradually declines with increasing distance downstream to about 13 mm and then rapidly shifts from gravel to sand across the remainder of Upper Reach 1, with few patches of fine gravel present to downstream of the Marine Drive Bridge at RM 2. The abrupt shifts in grainsize far exceed typical rates of downstream fining due to abrasion during transport and so suggest that sorting processes dominate the downstream reduction in grainsize. The gradual decline in grainsize across Lower Reach 3 and Reach 2 is lower than typical rates for sorting-dominated change in grainsize but substantially higher than typical rates for abrasion, suggesting relatively ineffective sorting processes dominate the downstream reduction in grainsize in that area.

Bank materials along the river can be divided into three broad zones. Upper Reach 3 and Lower Reach 4 have bank stratigraphy characteristic of migrating gravel bed rivers, with gravel along the base of the

bank from about the height of bars in the reach down to the depth of scour overlain by zero to 8 feet of sand (and sometimes silt) with generally increasing thickness of sand downstream. These banks have little to moderate stabilization from roots of riparian trees, which appear to generally increase in depth of stabilization with age of vegetation, with the exception that the one observation of late-seral Mixed Riparian Forest had lower depth of root stabilization than mature early-seral cottonwood forest due to the relatively shallow rooting depth of the coniferous trees in the Mixed Riparian Forest. Regime assessment suggests that the reach-scale bank strength contribution from forest in Reach 4 and Upper Reach 3 is negligible (μ values of 1.01 to 1.05). Bank conditions in Reach 2 and Lower Reach 3 are dominated by material that is not Nooksack River alluvium including recessional glacial outwash, which is only locally exposed in filled paleo channel cuts through surrounding fine-grained alluvium interpreted to have been deposited in a low energy floodplain or lacustrine environment. The outwash is poorly indurated while the fine-grained material is cohesive, resulting in substantially higher natural bank strength along this portion of the river. Few exposed banks were noted through Reach 1, which flows through the river's recently-formed delta. The native material in these banks can be inferred to be material deposited in that delta environment.

Select local hydraulic controls modulate the overall downstream trend of declining shear stress, and therefore the overall pattern over sediment mobility. The most important of these are constructions that form upstream backwaters with low shear stress during flood events. These occur at the lower edge of Upper Reach 3, at the just downstream of the Guide Meridian Bridge in Upper Reach 2, and at Main Street in Ferndale. Of these, the connection to change in channel morphology and grain size is strongest at the site in Upper Reach 3, suggesting that this location is the key capacity limitation for the Lower River and area where the channel likely shifts from a capacity-limited transport condition to a supply limited condition. This is likely a region of substantial movement of coarse sediment into long-term storage, potentially driving channel aggradation. The pinch point just below Guide Meridian is formed by levee restriction of overbank flow, while the constriction at Ferndale results from a combination of Pleistocene sediment and bridge infrastructure. Both of these produce strong upstream backwaters and shear stress reversal during higher floods but have little observable impact on the channel morphology, suggesting that common flows have the capacity to move material that might accumulate during larger floods.

There is a fundamental break in processes controlling channel morphology that occurs near the boundary between Upper and Lower Reach 3. This change is interpreted as a legacy of the Late-Holocene avulsion of the Nooksack River into its present course towards Bellingham Bay. Below this point, channel migration following the avulsion has been limited enough to prevent establishment of alluvial conditions along the river. Upper Reach 3 is below the avulsion node, but here channel migration has established alluvial banks along the river. Declining slope combined with the relatively (compared to downstream reaches) wide channel through Upper Reach 3 results in low shear stress, likely driving sedimentation. Lower Reach 4b and 4c are interpreted to have initially degraded following the avulsion and may now be in a near-equilibrium or potentially slightly aggradational condition. Lower Reach 4a and the downstream portion of Upper Reach 4, in contrast, have relatively high shear stress and coarse bed material, which may be a signal of upstream propagating degradation following the avulsion.

Regime analysis suggests that the present cross-sectional channel morphology in Lower Reach 3 and areas downstream is relatively insensitive to the past human modifications, while Reach 4 and Upper Reach 3 have both been highly impacted by human activities and have the potential to respond to future management. The effect of bank hardening has not yet caused wholesale change at the reach scale, but because of the huge change from naturally low bank strength conditions, it has the potential to have strong local morphologic impacts and would —if expanded— have the potential to radically alter the channel morphology. Historic removal of in channel wood has likely been the largest other anthropogenic impact through Reach 4. The regime predicted widths are substantially lower than historic channel belt widths in this area suggesting that stable large wood jams played a governing control by splitting flow into anabranching channels in this area.

TABLE OF CONTENTS

1	INTRODUCTION	1
2	CHANNEL HYDRAULICS.....	1
2.1	Hydraulic Model	1
2.2	Summary Hydraulic Profiles	2
2.3	Unsteady Hydraulic Conditions and Local Hydraulic Variability.....	5
2.3.1	Upper Reach 4	5
2.3.2	Lower Reach 4	10
2.3.3	Reach 3	12
2.3.4	Reach 2	15
2.3.5	Reach 1	18
3	BED AND BANK MATERIAL	21
3.1	Existing Data	21
3.2	Field Observations	22
3.2.1	Bed Material	23
3.2.2	Bank Material and Vegetation Stabilization of Eroding Banks	25
4	SEDIMENT MOBILITY PATTERN	30
5	REGIME AND PLANFORM GEOMETRY.....	33
5.1	Bank Strength	34
5.2	Channel Forming Discharge.....	36
5.3	Slope	36
6	KEY LARGE-SCALE PROCESSES CONTROLS GOVERNING CHANNEL MORPHODYNAMICS.....	37
	REFERENCES.....	37

LIST OF TABLES

Table 1: Peak main channel discharge at select cross sections for scaled flood peak model runs.	2
Table 2: Calibrated parameterization for UBCRM Calculations.....	34
Table 3: Summary of estimated changes in channel slope and corresponding change in width.....	36

LIST OF FIGURES

Figure 1: Summary of flood-flow hydraulic conditions along the Lower Nooksack River.	4
Figure 2: Water surface slope and shear stress hysteresis loops for 2-yr flood simulation at select locations.	6
Figure 3: Water surface slope and shear stress hysteresis loops for 100-yr flood simulation at select locations.	7
Figure 4: Depth and shear stress maps for Upper Reach 4.	8
Figure 5: Depth and shear stress maps for Upper Reach 4 and Lower Reach 4a.	9
Figure 6: Depth and shear stress maps for Lower Reach 4b and 4c.	11
Figure 7: Depth and shear stress maps for Upper Reach 3.	13
Figure 8: Depth and shear stress maps for Lower Reach 3.....	14
Figure 9: Depth and shear stress maps for Upper Reach 2.	16
Figure 10: Depth and shear stress maps for Lower Reach 2.....	17
Figure 11: Depth and shear stress maps for Upper Reach 1.	19
Figure 12: Depth and shear stress maps for Lower Reach 1.....	20
Figure 13: KWL’s (2008) model of channel bank material composition.....	21
Figure 14: WY 2017 Hydrograph for Nooksack River at North Cedarville.	22
Figure 15: Summary of bed material grainsize data along the Nooksack River.	24
Figure 16: Thickness of upper bank sand or silty sand and lower bank gravel or cobble-gravel bank stratigraphic units.	25
Figure 17: Observed pattern of bank conditions (bottom) and facies distribution in eroding banks (top).	26
Figure 18: Depth of observed root stabilization by age of bank top vegetation.....	29
Figure 19: Comparison of channel hydraulics with bed material grainsize illustrating along-channel variability in sediment mobility.....	31
Figure 20: Summary of UBCRM calculations illustrating channel sensitivity to varying bank strength and channel forming flow.	35

LIST OF PHOTOGRAPHS

Photo 1: A characteristic example of cutbacks in Reach 4 showing floodplain sand overlying gravel. Also not the limited stabilization from the roots of this immature cottonwood stand.	27
Photo 2: Example of recessional glacial outwash exposed in a Nooksack River Cutbank.	28

Photo 3: Fine consolidated grained silt and clay with abundant wood and organic material characteristic of banks through Reach 2 and potentially Lower Reach 3..... 28

Photo 4: Moderately deep root stabilization provided by Mature Mixed Riparian Forest. 29

1 INTRODUCTION

This report describes results of NHC’s observations and calculations related to hydraulic conditions, bed and bank material, sediment mobility, and regime analysis along the Lower Nooksack River. Considerable previous work —and accompanying analysis— document the present and historical planform geometry of the channel, the geologic context of the channel, and floodplain geomorphic conditions, while others have modeled hydraulic conditions along the river, primarily for flood inundation mapping and floodplain management planning.

The present study aims to understand principal habitat-forming geomorphic processes along the river. Other components of the study are focused on understanding channel morphodynamics, controlling geologic history, and floodplain vegetation interactions. This component brings together observations of geomorphic conditions in the channel, modeled channel hydraulics, and information on the channel bed and bank materials to quantify key physical fundamental geomorphic processes that control the cross-section and profile geometry of the river.

The memo focuses on direct reporting of observations, calculations, and methods applied, in the anticipation that interpretation of these results will be included in the main report for the project. Sections 2 and 3 present data describing channel hydraulics and boundary material, respectively, with limited commentary on key river management implications. These data are integrated in Sections 4 and 5, which explore sediment mobility patterns and controls on channel cross-section geometry, respectively; these sections begin to explore the river management implications of the hydraulic and boundary material data. Finally, in conclusion, Section 6 describes—a the river system scale— process controls governing channel morphodynamics. Reach definitions and river mile stationing conventions are the same as those adopted in Table 1 of the accompanying main report.

2 CHANNEL HYDRAULICS

2.1 Hydraulic Model

The existing one-dimensional Full Equations (FEQ) hydraulic model of the Lower Nooksack River was developed primarily for the goal of mapping inundation extents for relatively low-recurrence interval floods (Linsley, Kraeger Associates, Ltd., 2004). The present iteration of the model utilizes bathymetry data collected in 2006 and calibration against flood water levels.

In order to better reflect conditions during more frequent channel forming flood flows, the model was run for scaled hydrographs representing 2-, 5-, 10-, 25-, 50-, and 100-year flows (Table 1) without applying the invert-lowering calibration. The downstream base level control for these model runs was a mean lower low water condition, and so hydraulic conditions imposed by tidal backwater along the lower four miles of the channel are not represented. Two kinds of model results were provided to NHC:

- 1) Summary tables showing the peak stage reached at each model cross-section along the river (and floodplain flow paths), and
- 2) Special output tables showing the stage and discharge hydrographs at selected pairs of cross-sections at key sites along the river.

Hydraulic results in the summary tables were mapped over recent (Anderson and Grossman, 2015) bathymetry data and extrapolated into continuous two-dimensional grids of water surface elevation, depth, water surface slope, and shear stress —computed as the depth slope product ($\rho g h s$)— across the active channel. Because the hydraulics were only computed in a one-dimensional model, these two-dimensional plots provide a relatively coarse approximation of real conditions across the channel. The local accuracy of this extrapolation is probably higher for larger events as across-channel hydraulic variability is reduced. The model input geometry substantially pre-dates the topobathymetric surface onto which the outputs were mapped. This will produce inaccuracies in areas of substantial geomorphic change to the extent that the channel hydraulics would have changed between the 2006 and recent topography. In areas of aggradation, water depth (and therefore shear stress) will tend to be underestimated, while in areas of degradation, depth may be overestimated.

Table 1: Peak main channel discharge at select cross-sections for scaled flood peak model runs.

Reach	XSID	Q_{max} (ft ³ /s)*					
		2-yr	5-yr	10-yr	25-yr	50-yr	100-yr
Lower Reach 1	RAXSZB	22,378	26,168	27,731	28,484	28,692	28,959
Middle Reach 1	RAXSZP	22,628	26,791	27,524	27,998	28,820	29,398
Upper Reach 1	RAXSAI	22,752	31,506	39,419	45,547	51,428	54,799
Lower Reach 2	RBXSBB	20,960	21,792	22,034	22,537	22,867	23,338
Upper Reach 2	RBXSAS	23,641	24,041	24,668	24,338	24,929	25,033
Lower Reach 3	RCXSAP	32,605	38,517	40,975	42,379	42,653	43,073
Upper Reach 3	RCXSEG	33,292	40,722	47,488	54,776	56,409	58,212
Lower Reach 4c	RDXSAJ	33,398	40,920	48,711	60,718	65,278	73,232
Lower Reach 4a	RDXSBP	30,850	39,341	46,492	56,748	62,588	70,104
Upper Reach 4	RDXSFJ	30,450	40,723	48,487	58,405	65,922	74,487

* Note that Q_{max} varies along the channel due to floodplain flow. Flow in Upper Reach 1 and Upper Reach 4 are approximately the total river discharge at those points.

2.2 Summary Hydraulic Profiles

Hydraulic conditions along the channel thalweg were extracted from the mapped summary hydraulic outputs for each flood event described above. Figure 1 shows resulting profiles. The channel bed profile (bottom plot) is distinctly concave, and flood water surface slopes correspondingly decline in the downstream direction, dropping by an order of magnitude from a typical slope of about 0.3% in Upper Reach 4 to 0.02% in Upper Reach 1. The increase in slope from Upper Reach 1 to Lower Reach 1 occurs because the model was run with a low-tide downstream boundary condition. The decline along the river,

however, is neither monotonic nor consistent for the range of modeled flood events due to the formation of backwaters above localized constrictions.

Channel depth also generally increases in the downstream direction. During the 2-year flood, typical depths increase by a factor of two from 10-12 feet in the upstream portion of Lower Reach 4 (no current thalweg depth data are available for Upper Reach 4) to 20-25 feet in Lower Reach 2 and Upper Reach 1. Shear stress—a measure of energy available to transport bed material—is computed as the product of depth and slope and so the increasing depth in the downstream direction partially counteracts the decrease in slope. However, because the slope decreases more than depth increases, typical channel shear stress also decreases in the downstream direction. During a 2-year flood, it drops from greater than 100 Pa upstream to approximately 20 Pa through Upper Reach 1. For reference—assuming a τ^*_c value of 0.03 (See Section 4)—100 Pa is capable of transporting medium-sized cobble while 20 Pa is capable of moving only relatively fine (<45 mm) gravel.

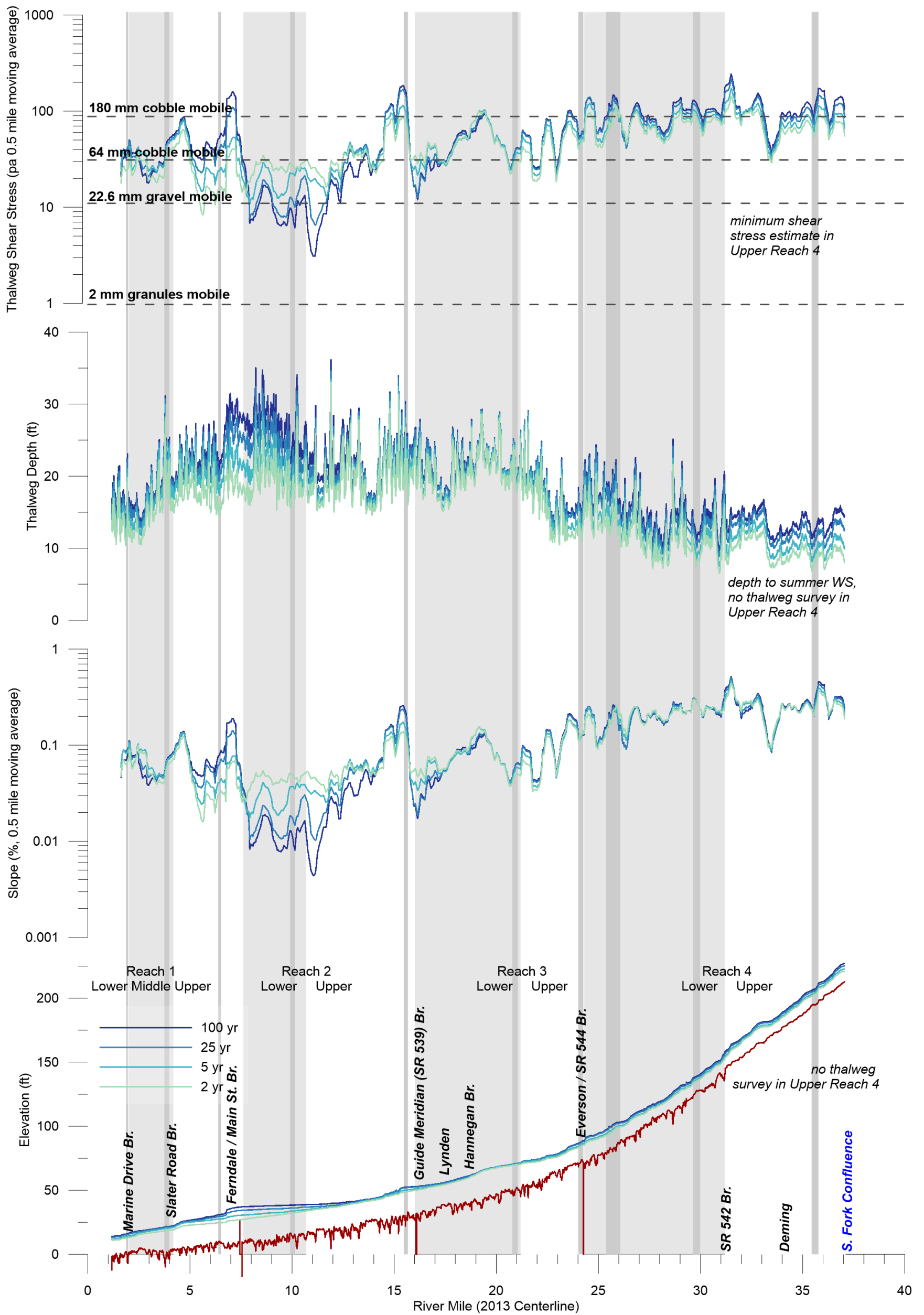


Figure 1: Summary of flood-flow hydraulic conditions along the Lower Nooksack River. Note: competence calculations for gravel mobility assumed τ^*_c of 0.03. Dark bands indicate the position of special output evaluation for full flood hydrographs.

2.3 Unsteady Hydraulic Conditions and Local Hydraulic Variability

The plots and description of the overall channel profile and accompanying hydraulic conditions described above obscure important unsteady hydraulic conditions and local hydraulic variability. Special output for flood hydrographs was evaluated at select locations to show the impact of unsteady hydraulics and inform the following discussion of key hydraulic controls in each sub reach.

Figure 2 and Figure 3 show hysteresis loops for water surface slope and thalweg shear stress for each of the special output locations over the course of 2- and 100-year floods, respectively. These plots illustrate how in some areas, slope and shear stress increase with increasing discharge, while in others, a decrease in slope due to the formation of backwater ponding results in a drop in shear stress at high flows.

2.3.1 Upper Reach 4

In Upper Reach 4, shear stress is competent to move small cobble-sized material during flow exceeding about 10,000 cfs (Figure 2 and Figure 3) and can locally move large cobble at the 2-yr flow throughout the reach (Figure 2, Figure 4 and Figure 5). At the selected special output location, the water surface slope increases with increasing discharge to about 20,000 cfs and then levels out, producing substantial convexity but a monotonic increase of shear stress with increasing flow. A localized dip in water surface slope and shear stress occurs at RM 34, where hydraulic conditions at the time the FEQ model was developed may have differed substantially from those at the present due to control from the Clay Banks landslide just downstream at RM 33.

The SR 542 bridge crosses a notably narrow location relative to the surrounding channel. The narrow channel at this location is mostly driven by deep scour along the left bank revetment, and is not due to a constriction from the bridge. Shear stress is consistently high just upstream of and through the bridge opening.

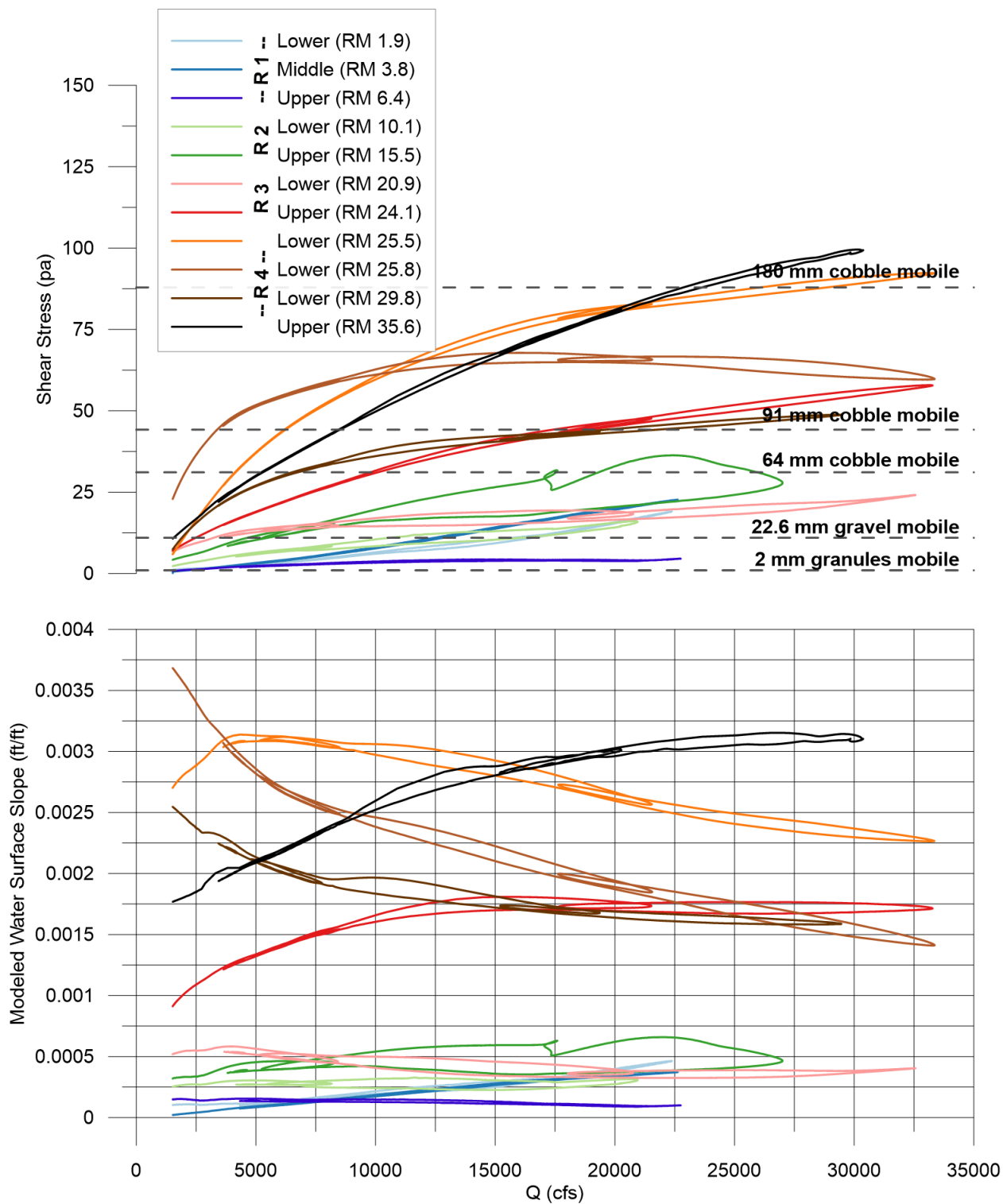


Figure 2: Water surface slope and shear stress hysteresis loops for 2-yr flood simulation at select locations. Grainsize competence thresholds assume $\tau^*_c=0.03$.

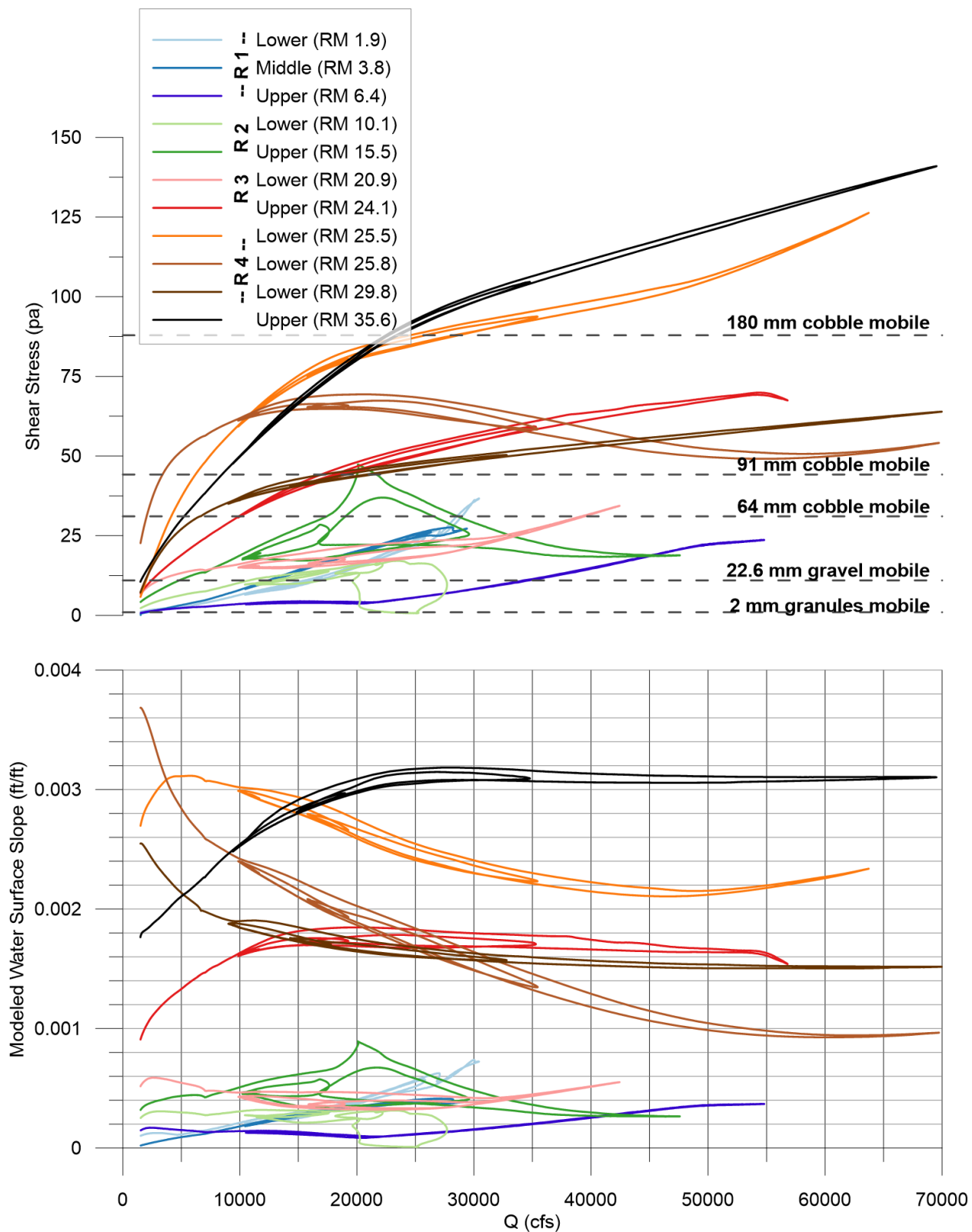


Figure 3: Water surface slope and shear stress hysteresis loops for 100-yr flood simulation at select locations. Grainsize competence thresholds assume $\tau^*_c=0.03$.

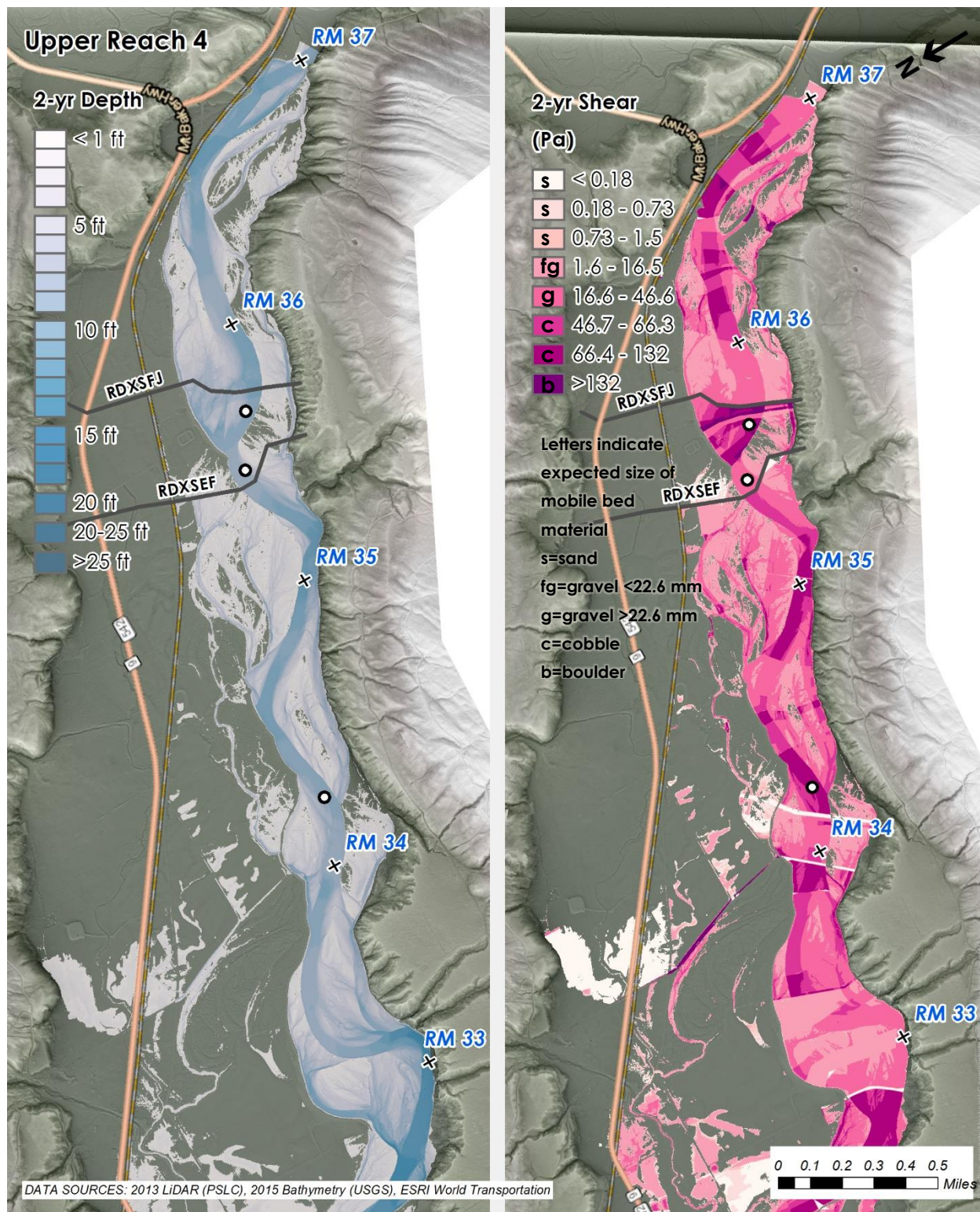


Figure 4: Depth and shear stress maps for Upper Reach 4. The 2015 USGS bathymetry does not extend into this area; depth is to the low-flow water surface and shear stress underestimated. Pebble count locations (circles) and special output cross-sections are indicated.

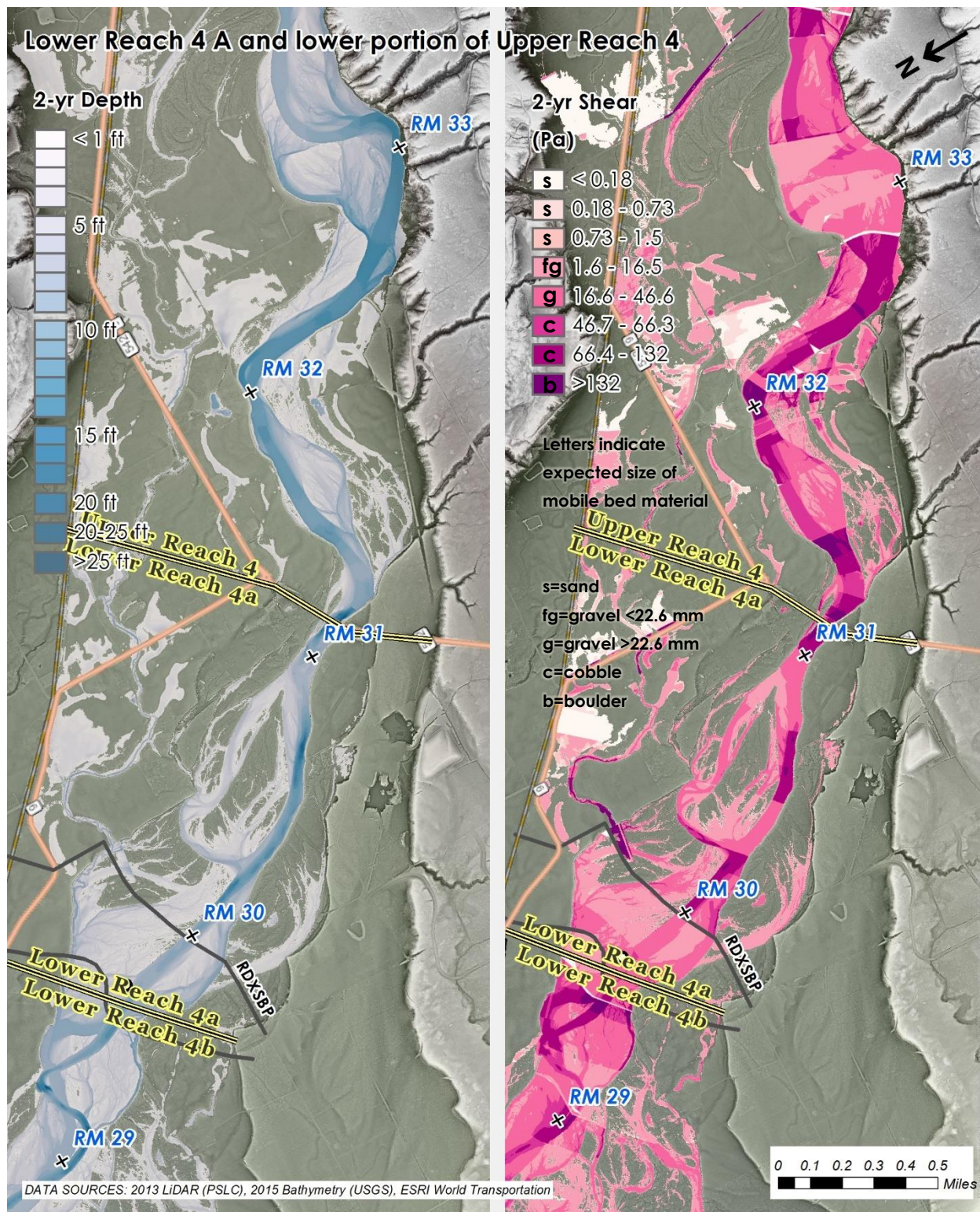


Figure 5: Depth and shear stress maps for Upper Reach 4 and Lower Reach 4a. The 2015 USGS bathymetry does not extend above SR 542; depth is to the low-flow water surface and shear stress underestimated. Pebble count locations (circles) and special output cross-sections are indicated.

2.3.2 Lower Reach 4

Shear stress along Lower Reach 4 during the 2-yr flow is generally in the range of 45 to 130 Pa, which is competent to move small to medium-sized cobbles (Figure 5 and Figure 6). Because of the very wide channel, depth does not increase appreciably with increasing flood magnitude and there is a narrow band of shear stress from the 2- to 100-year recurrence interval flow (Figure 1).

Due to high along-channel variability and potentially complex interactions between discharge and shear stress in Lower Reach 4, three locations were selected for evaluation of special output over the duration of the flood hydrographs. The most upstream of these locations occurs at about the upstream boundary of Lower Reach 4b, where the active channel width increases substantially in the downstream direction. The FEQ output at this location (RM 29.8) shows a monotonic decrease in slope with increasing discharge and consequently slow increase in shear stress with increasing discharge. Hydraulic conditions at this site have probably changed due to channel migration since the FEQ model was developed, and so this pattern may not accurately reflect existing conditions.

The lower two special output locations were located just above (RM 25.8) and spanning (RM 25.5) the “funnel” where the active channel and flow zone become increasingly constricted as the river approaches the Everson Road Bridge (Figure 6 and Figure 7). Both sites show pronounced declines in water surface slope with increasing discharge (Figure 2 and Figure 3), and the upstream site occurs at a substantial local shear stress minima. Furthermore, the maximum shear stress at this location occurs at a fairly low flow of about 20,000 cfs. The water surface slope is uncharacteristically steep for the reach through the funnel, resulting in high shear stress in the reach approaching the bridge.

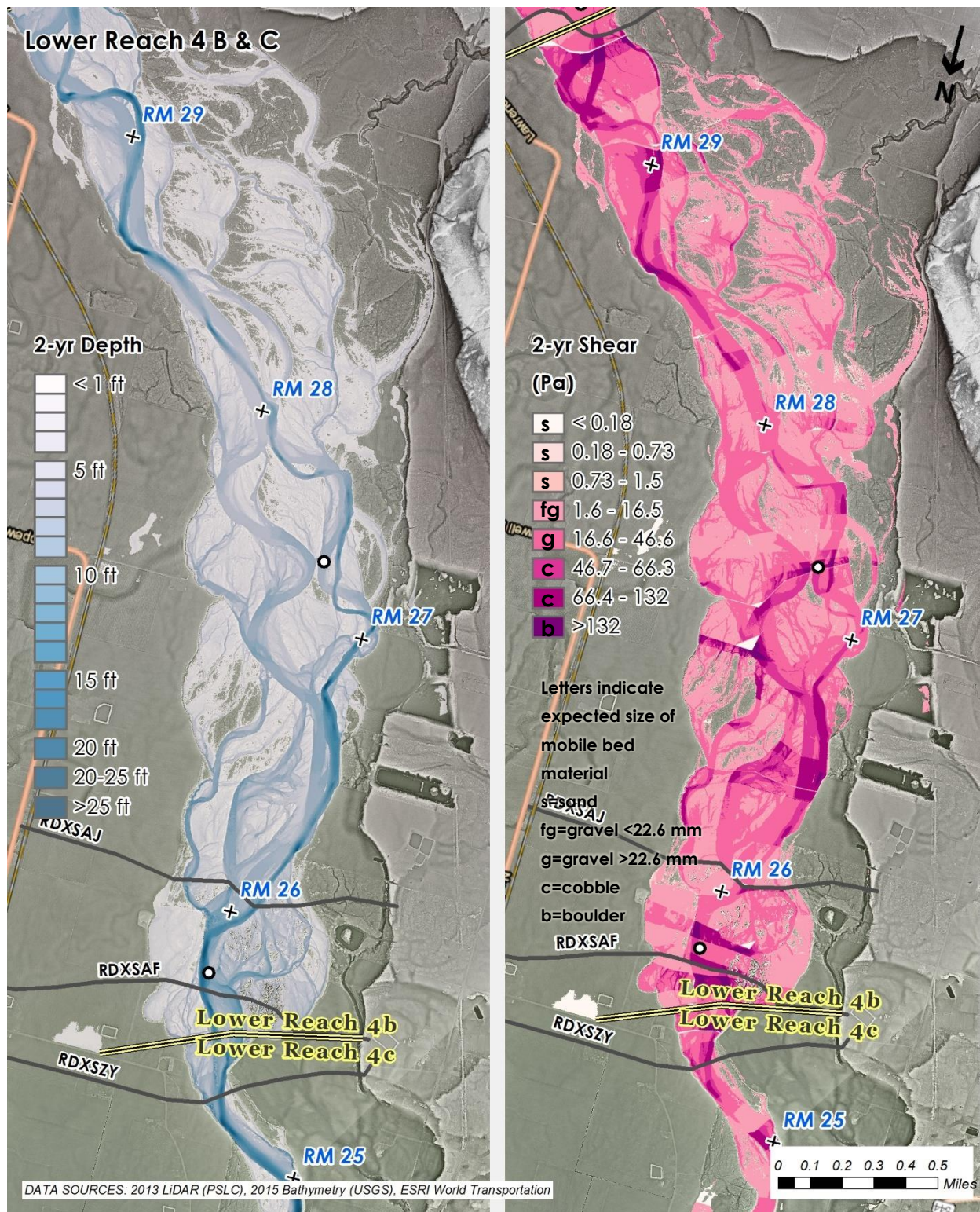


Figure 6: Depth and shear stress maps for Lower Reach 4b and 4c. Pebble count locations (circles) and special output cross-sections are indicated.

2.3.3 Reach 3

Shear stress consistently declines from over 100 Pa passing through the Everson Bridge upstream to approximately 25 Pa at the downstream limit of Upper Reach 3 (Figure 1). Just below the Everson Bridge (RM 24.1), shear stress is comparable to that observed through Reach 4. Water surface slope has a maxima around 15,000 to 25,000 cfs and declines very slightly for much larger flows, while shear stress increases nearly monotonically with increasing flow (Figure 2 and Figure 3). The decline in shear stress from upstream to downstream across Reach 3 is robust across the whole range of flows. This is shown by substantial separation between shear stress across the whole range of flows from the Upper Reach 3 special output location —and all sites upstream— and the Lower Reach 3 special output location —and all sites downstream in Figure 2 and Figure 3.

The upstream boundary (head) of Lower Reach 3 (including the RM 20.9 special output location) occurs at a local shear stress minima (Figure 1) where the active channel is relatively wide, levees set back from the top of the bank, and water surface slope relatively gentle. Downstream of this, shear stress increases rapidly where levees confine the flow to a narrow corridor resulting in flow that is both relatively steep and deep along the lower portion of the Abbott levee. At this location, slope remains approximately constant across the range of flood flows, and so shear stress increases proportionally to depth (Figure 2 and Figure 3).

Although there is relatively little interaction between the channel and surrounding floodplain during the 2-year recurrence flow in this area, Lower Reach 3 marks the beginning of the river corridor where the Nooksack is perched on an alluvial ridge and escaping flood flows fill (and are conveyed through) flood basins along the valley margins, reducing the amount of flow conveyed by the main channel.

A major shear stress minima and site of ponding and shear stress reversal during larger floods occurs just below the downstream limit of Lower Reach 3 and is described in the following section. It impacts hydraulic conditions into the lower portion of Reach 3.

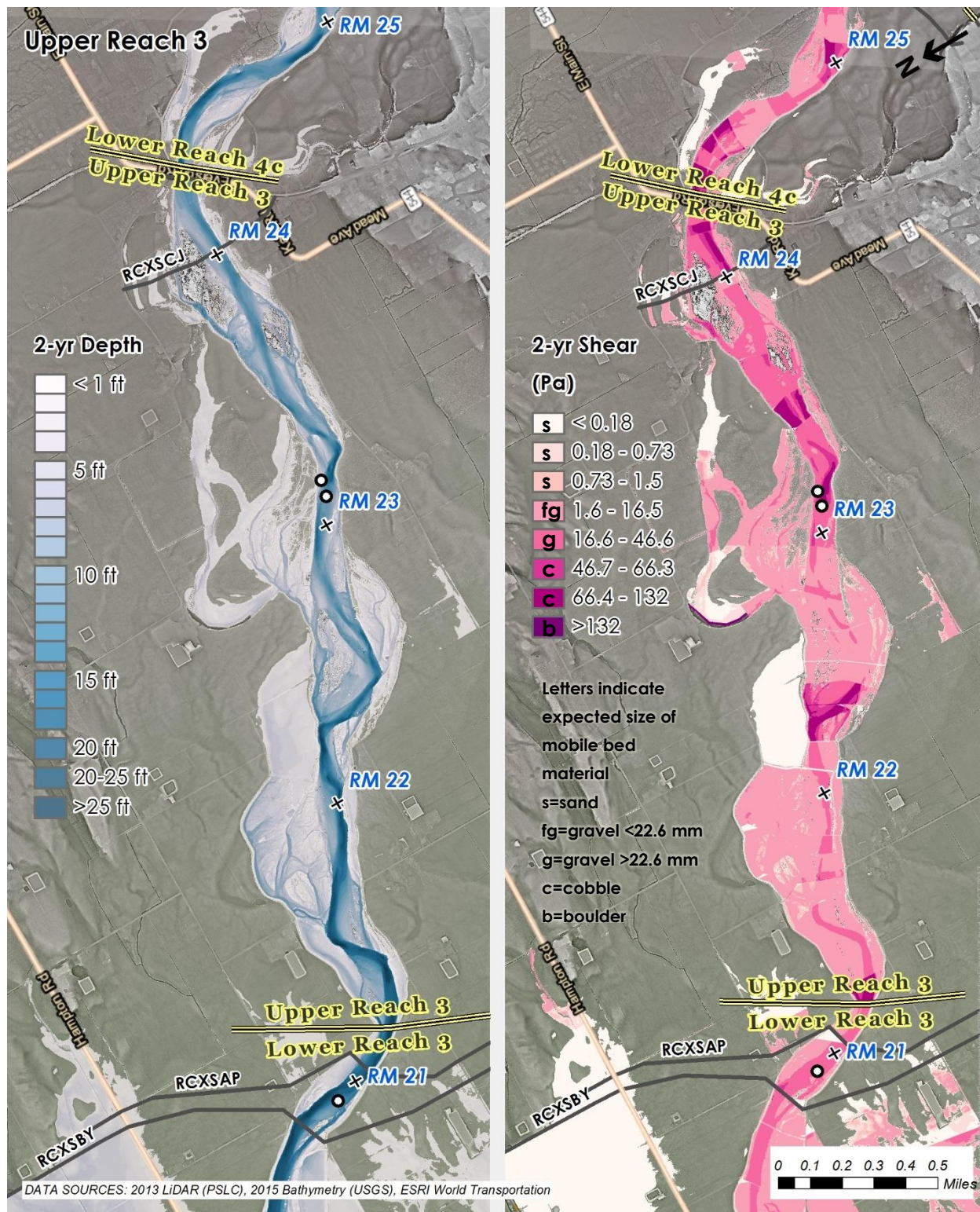


Figure 7: Depth and shear stress maps for Upper Reach 3. Pebble count locations (circles) and special output cross-sections are indicated.

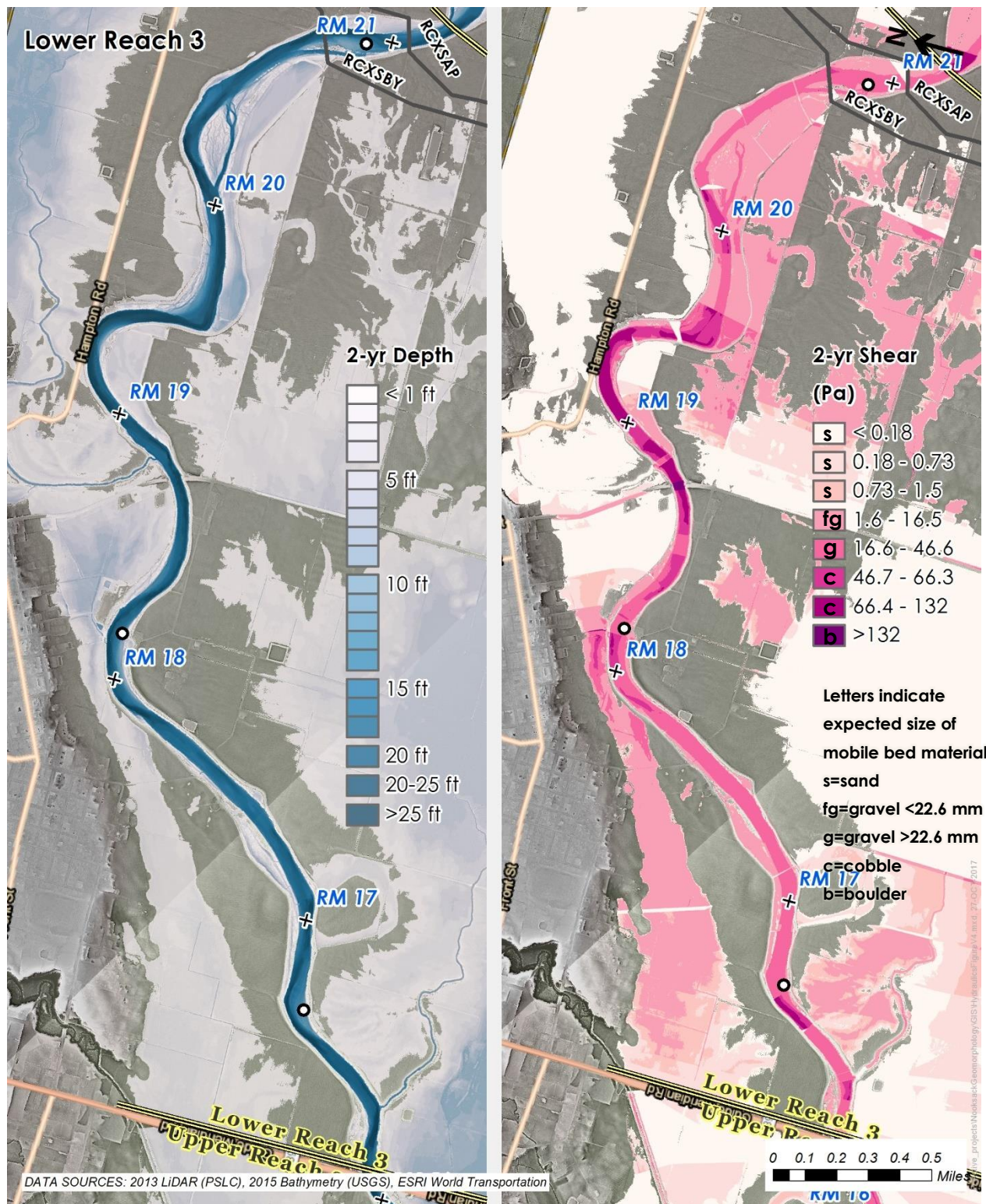


Figure 8: Depth and shear stress maps for Lower Reach 3. Pebble count locations (circles) and special output cross-sections are indicated.

2.3.4 Reach 2

Reach 2 extends from the Guide Meridian Bridge over the Nooksack River to the I-5 bridge over the river. Two major shear stress minima occur in the reach, one just downstream of the Guide Meridian Bridge and another that spans all of Lower Reach 2. In between the two minima, there is a zone of elevated shear stress that increases rapidly upstream and then declines gradually through the remainder of Upper Reach 2 (Figure 1).

The shear stress minima at the head of the reach is forced by a very substantial constriction at RM 15.3. This constriction is formed by naturally high ground to the south (and slightly exaggerated by the Vanderpool Levee to the south) and the River Road Levee to the north, which —along with the levee system upstream and around Fishtrap Creek— prevents flow conveyance through the large flood basin to the north of the channel. At this site (special output for RM 15.5), complex hysteresis loops occur where shear stress is generally higher during the rising limb of floods and lower during receding limbs (Figure 2 and Figure 3). During both the 2-yr and 100-yr hydrographs, the maximum shear stress occurs during the rising limb of the flood at about 20,000 cfs. During large floods, the water surface slope and shear stress upstream of the constriction decline substantially at flows greater than about 25,000 cfs.

A region of high shear stress (~ 100 pa) occurs in and below the constriction where flood flows escape into the left bank floodplain (Figure 9), resulting in a very steep local gradient (Figure 1). The water surface slope —and correspondingly shear stress— declines from this maxima to about the transition from Upper Reach 2 to Lower Reach 2, where the backwater from the constriction at Ferndale begins to affect channel hydraulics during larger floods.

During larger floods, formation of a pronounced backwater above the constriction at Ferndale (Figure 1) causes the slope and shear stress in Lower Reach 2 to drop with increasing flood magnitude, such that during the 100-year flood peak the minimum shear stress along the channel in Lower Reach 2 drops to about 3 Pa, which is only competent to move granule-sized sediment and finer; during a large portion of the 100-year flood duration, the slope and shear stress go to near zero (Figure 3). The surveyed bed profile does not reflect this water surface slope impact (Figure 1) and larger sediment is transported downstream, indicating that the sediment delivered to this backwater during larger floods is —in fact— readily flushed downstream during flood recession and/or subsequent smaller events when shear stress is higher (e.g. Figure 2).

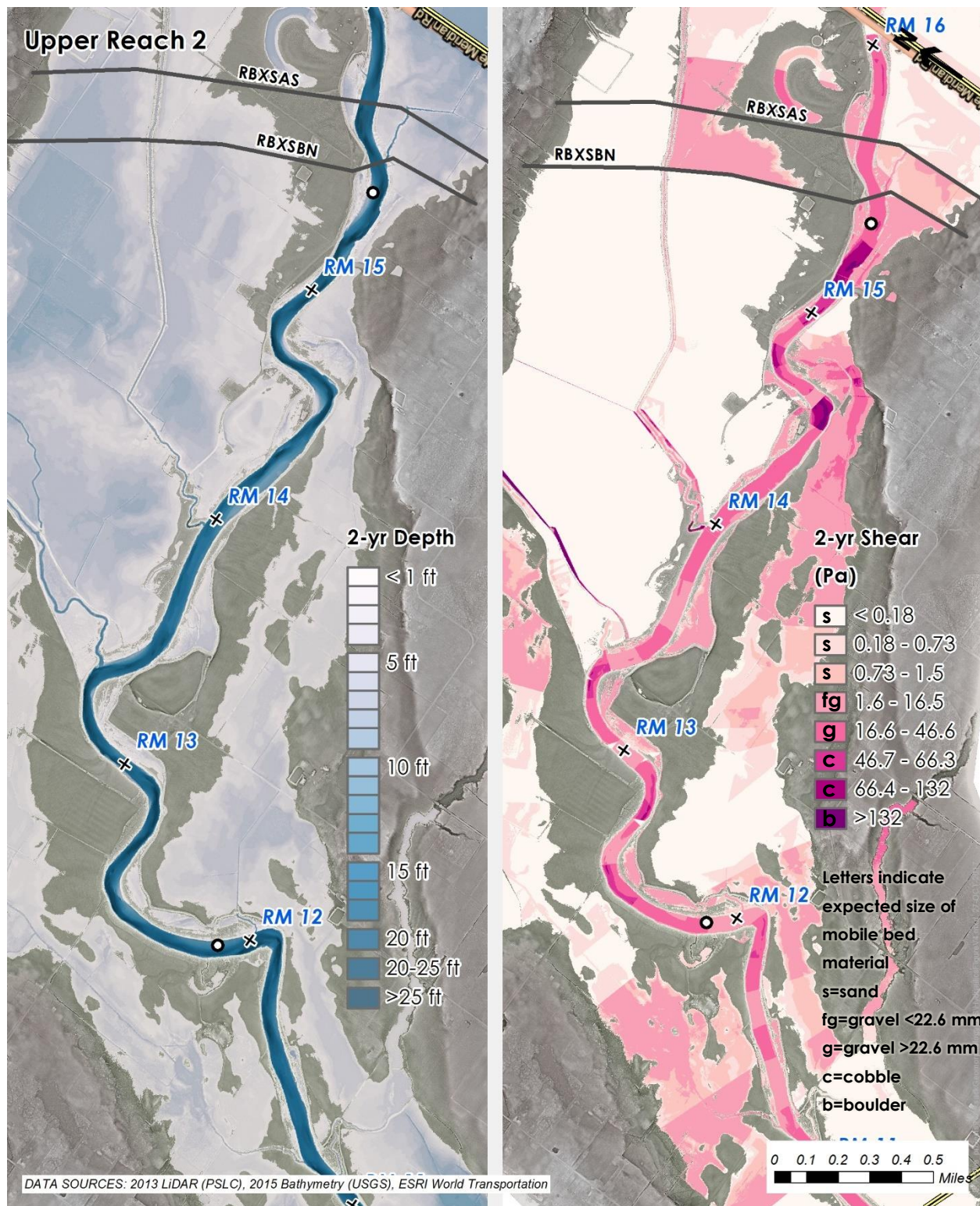


Figure 9: Depth and shear stress maps for Upper Reach 2. Pebble count locations (circles) and special output cross-sections are indicated.

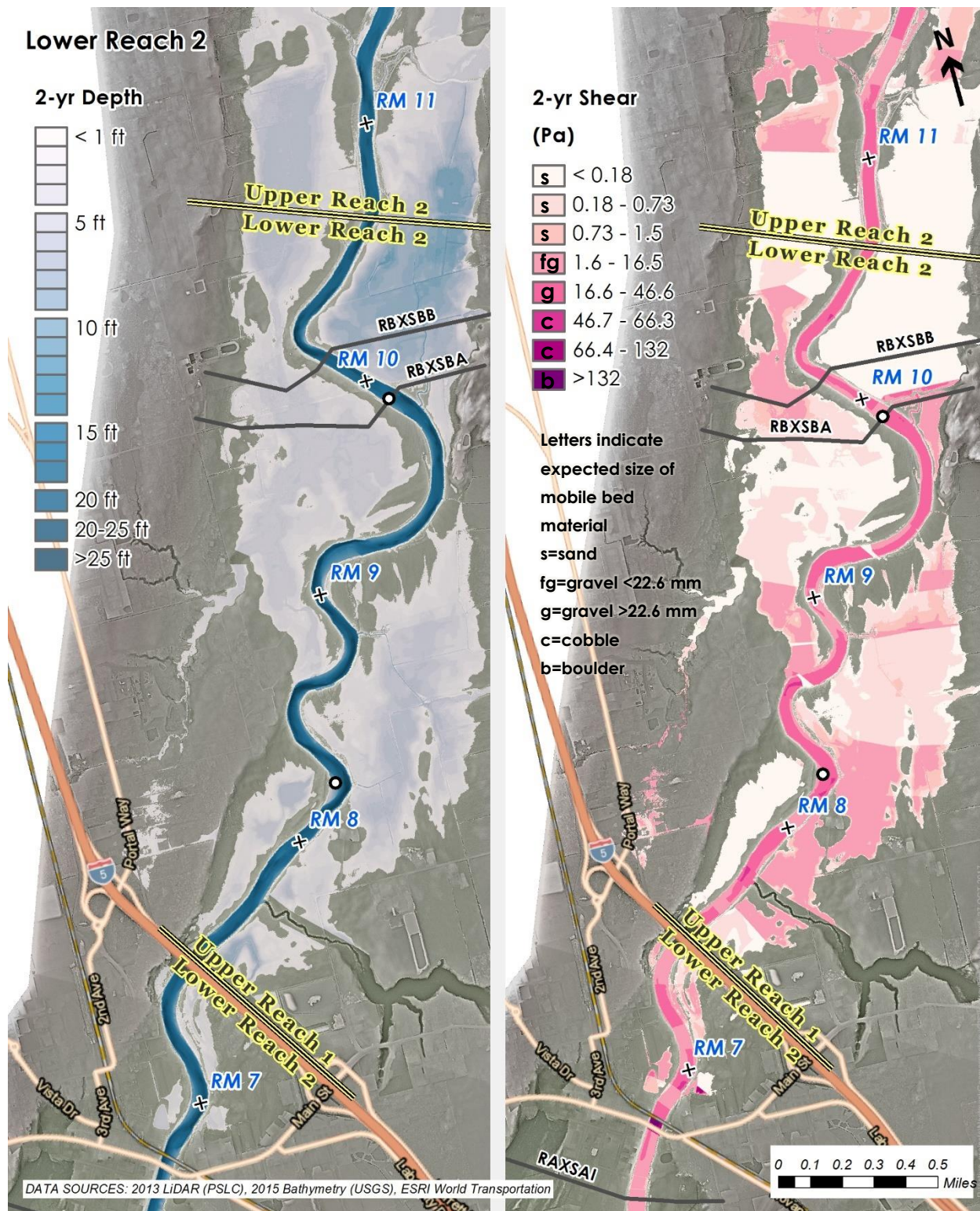


Figure 10: Depth and shear stress maps for Lower Reach 2. Pebble count locations (circles) and special output cross-sections are indicated.

2.3.5 Reach 1

The constriction at Ferndale at the head of Upper Reach 1 is formed where the combined influence of naturally high ground and a corridor of three bridges prevent floodplain flow around the channel (Figure 11). Slope, depth, and —therefore— shear stress, are all high through this constriction (Figure 1) but abruptly decline where the channel widens as it debouches from confining Pleistocene sediment into its late-Holocene delta at RM 6.5. Hydraulic model runs for this project were completed with a low-tide boundary condition, and so relatively steep slopes and high shear stress reflect the most severe hydraulic conditions expected in the reach. The total energy available for sediment transport likely reaches a minimum near the head of tidal impacts at the transition from Lower Reach 1 to Middle Reach 1 around the Marine Drive Bridge.

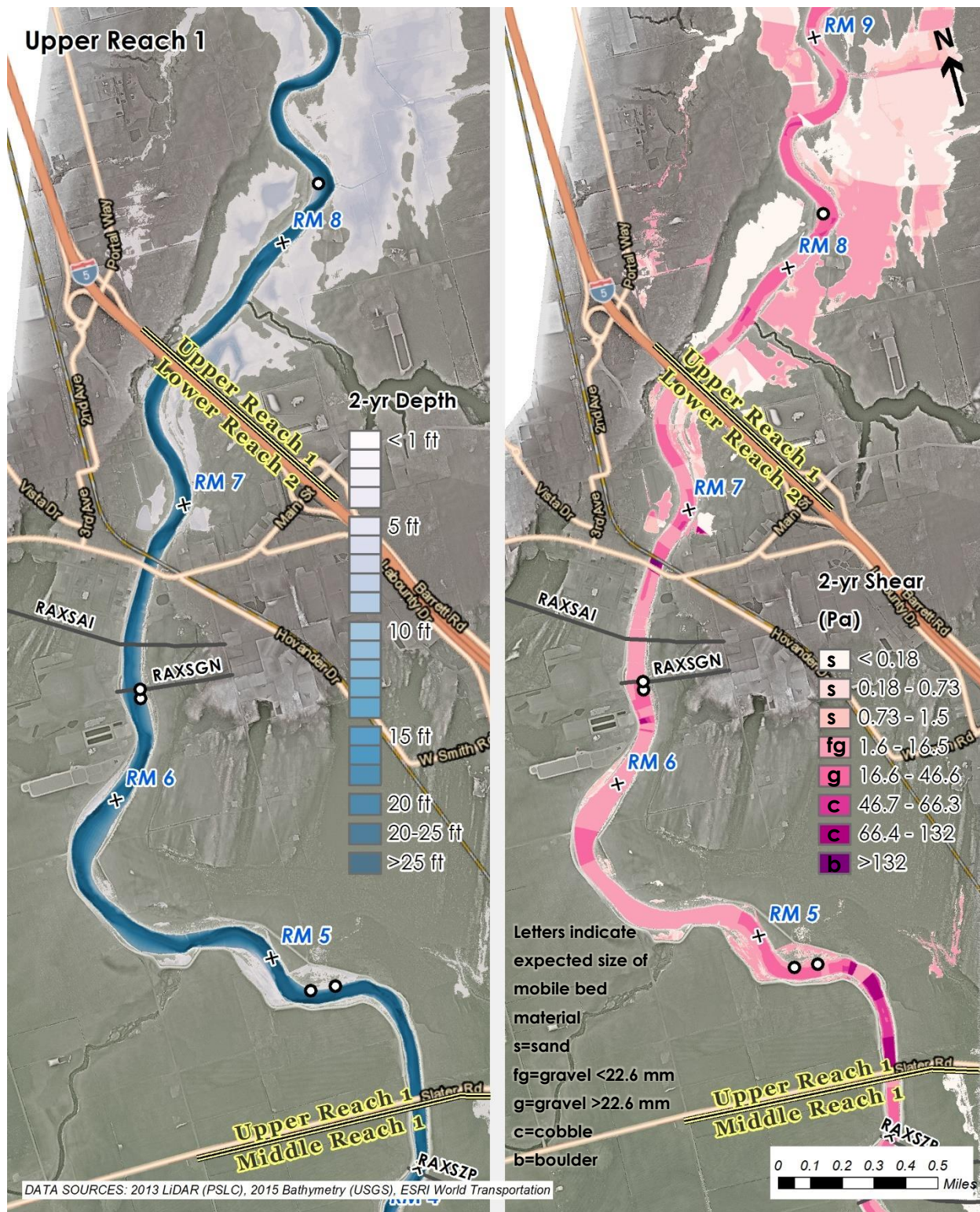


Figure 11: Depth and shear stress maps for Upper Reach 1. Pebble count locations (circles) and special output cross-sections are indicated.

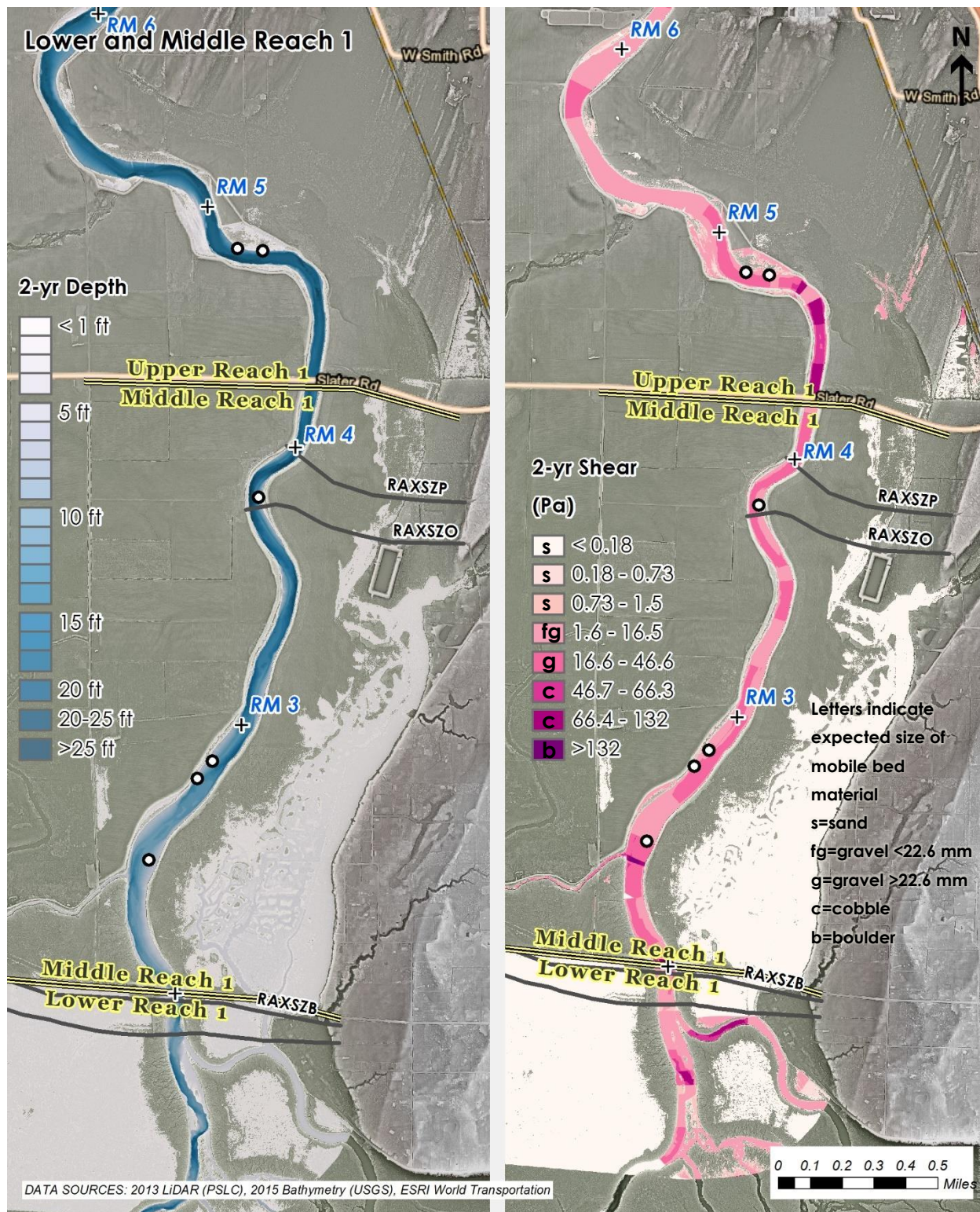


Figure 12: Depth and shear stress maps for Lower Reach 1. Pebble count locations (circles) and special output cross-sections are indicated.

3 BED AND BANK MATERIAL

In addition to channel hydraulics, the material of which the channel bed and banks are composed is a first order morphodynamic control. A thorough understanding of the bed and bank materials along the channel is, therefore, necessary in order to estimate sediment transport rates and understand controls on the channel's planform.

3.1 Existing Data

Two existing older datasets describe bed material along the river through the project reach: data collected by WEST in 1987 and data collected by KWL in 2005-2006 (reported in KWL, 2005). These datasets provide broad spatial coverage but pose three significant challenges for the present application. First, the along-channel stationing is somewhat ambiguous because the stationing maps utilized have not been located. Stationing was matched to the 2013 centerline used here by applying the same adjustment determined by NHC (2015). This is probably accurate to within about a mile or better. Second, enough channel change has occurred in many locations along the river that the surface texture from 1987, or even 2006, may not represent present-day channel hydraulics. Finally, it appears the previous investigators excluded grain sizes above 2" (50.8 mm). The way this coarser material was treated in the calculation of the cumulative grainsize distribution is not clear, and so reported grainsize data from any location where cobble composes a substantial portion of the channel bed is suspect. Cobble is present as a significant component of the channel bed from Upper Reach 3 upstream. In addition to these two older datasets, NHC (2015) collected sediment samples extending from approximately RM 6.2 to 2.5 and described bed material through the intervening reach. Locations of these samples are shown in Figure 11 and Figure 12.

Relatively little description of the channel bank material is available. KWL (2008) assumed a model of banks composed of alluvial gravel under 1.6 to 4.9 ft (0.5 to 1.5 m) of sand (Figure 13), which appears generally applicable through alluvial areas of Upper Reach 3 and Reach where channel banks are neither revetted nor intersecting the valley walls. Detailed specific observations follow in section 3.2.2.

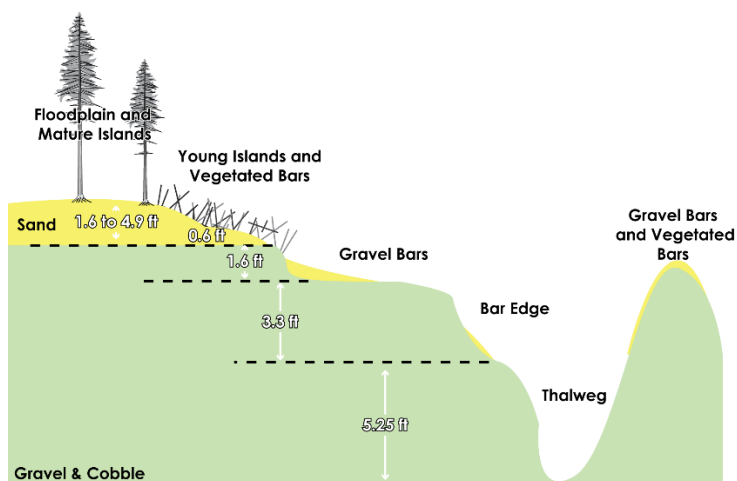


Figure 13: Sketch illustrating KWL's (2008) model of channel bank material composition.

3.2 Field Observations

Field observations of channel bed and bank material were collected during a float transect of the river from the South Fork Confluence to Ferndale boat ramp at RM 6.5 on July 31-August 1, 2017. Flow at the time of observation ranged from 1,800 to 2,000 cfs at the North Cedarville Gage (USGS 12210700) and followed a winter with relatively modest (<2 yr recurrence) flood flows (Figure 14).

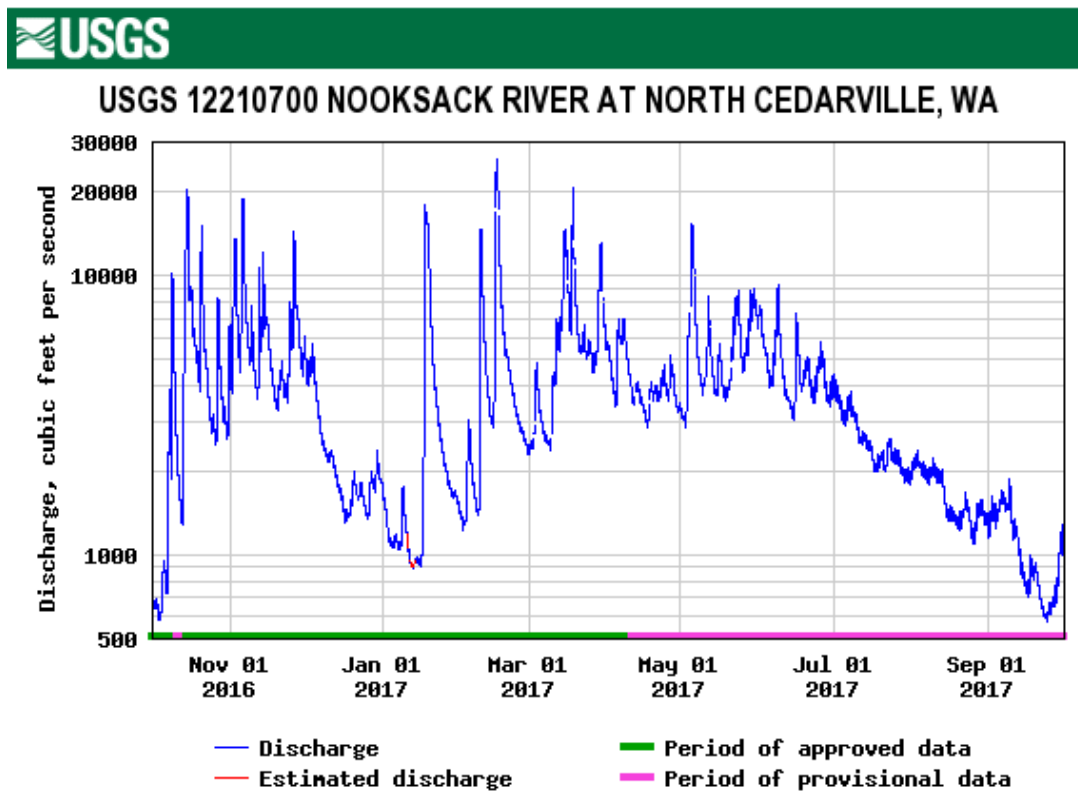


Figure 14: WY 2017 Hydrograph for Nooksack River at North Cedarville.

Pebble counts were conducted on bar-head locations that appeared typical of the surrounding channel following a random-walk Wolman (1954) procedure, with one to four people selecting stones for each count. The stratigraphy of cut banks was noted, with heights of each facies and degree of stabilization from riparian vegetation visually estimated.

In addition to pebble counts, the surface texture across each bar along the raft transect route was qualitatively categorized to provide indications of rapid shifts in grainsize distribution at a finer spatial scale than practical for pebble counts. This texture was estimated by visually categorizing the dominant and subdominant grainsize divided into groups according to the Wentworth (1922) classification system, with the exception that gravel was divided into only two subclasses denoted as “gravel” consisting of particles between 22 and 64 mm and “fine gravel” consisting of particles between 2 and 22 mm¹. The

¹ This use of “fine gravel” is not consistent with Wentworth’s “fine pebble” class which is restricted to particles smaller than 8 mm.

proportion of each facies was then estimated from these notes for each river mile. Data below the raft transect take-out location were filled in from notes associated with NHC's (2015) fieldwork along that reach.

3.2.1 Bed Material

Figure 15 shows a compilation of the available grainsize distribution data. There is a clear general downstream fining trend, with alternating zones of relatively rapid downstream fining and little to no downstream fining indicated by both the bar-head pebble count data and the facies distribution data.

A commonly used descriptor for the rate of downstream fining is the diminution coefficient α_d , which is simply defined as the rate of decline of grainsize per unit distance, traditionally reported in units of phi (Φ)/km. Between the coarsest sample at RM 34.2 and last pebble count above the gravel to sand transition at RM 6.4, the D_{84} declines from 116 mm to 21 mm and D_{50} declines from 74 mm to 13mm; so $\alpha_{d50} = 0.055 \Phi/\text{km}$ and $\alpha_{d84} = 0.057 \Phi/\text{km}$. This value is within —but on the low side of— the range for rivers where downstream fining is controlled by sorting processes, where values of $0.04 < \alpha_d < 1$ are typical and well above normal values for rivers dominated by abrasion, where values of $0.001 < \alpha_d < 0.01$ are typical (Rice, 1999). If downstream fining is controlled by sorting processes, then the largest particles in the river bed must be moving into long-term storage in the river or valley bottom, driving aggradation.

The general river-scale declining trend, however, is punctuated by regions of relatively fast downstream fining, where sorting processes must be particularly effective and relatively fast sediment accumulation may be inferred. There is little change in either the overall facies distribution or bar head grainsize distribution from the head of Upper Reach 4 downstream through Lower Reach 4c, but a rapid shift from cobble to gravel and cobble dominated bed material occurs near RM 29, where the river abruptly widens and emerges into the broad braided zone of Lower Reach 4b (Figure 5, Figure 6, and Figure 15). Between pebble counts at RM 29.7 and 27.3, D_{84} declines from 110 mm to 64 mm and D_{50} declines from 70 mm to 38 mm, resulting in α_{d50} and α_{d84} of 0.23 and 0.20, respectively.

Little change in the grainsize of bar-head locations selected for pebble counts occurs between RM 27.3 and the lower portion of Upper Reach 3 at RM 20.9, but the typical surface facies composition of bars along the channel does continue to fine somewhat in this area (Figure 15). Lower Reach 3 is a zone of persistent and monotonic downstream fining, with a substantial increase in the abundance of sand and a change in the bar-head D_{84} and D_{50} values from 71 mm to 42 mm and from 49 mm to 26 mm, respectively (comparing pebble counts at RM 20.9 and 15.3); the overall value of α_{d50} and α_{d84} across the sub reach are 0.10 and 0.08, respectively.

There is little change in the bar-head texture between pebble counts at the upstream edge of and in the middle of Upper Reach 2, with an α_{d50} value of about 0.04 and α_{d84} of 0.03. The area in between the pebble counts has a relatively high abundance of gravel and scarcity of fine gravel and sand in observed bars and locally high shear stress, suggesting that the limited downstream fining occurs because all bed material delivered to the sub reach from upstream is readily flushed downstream.

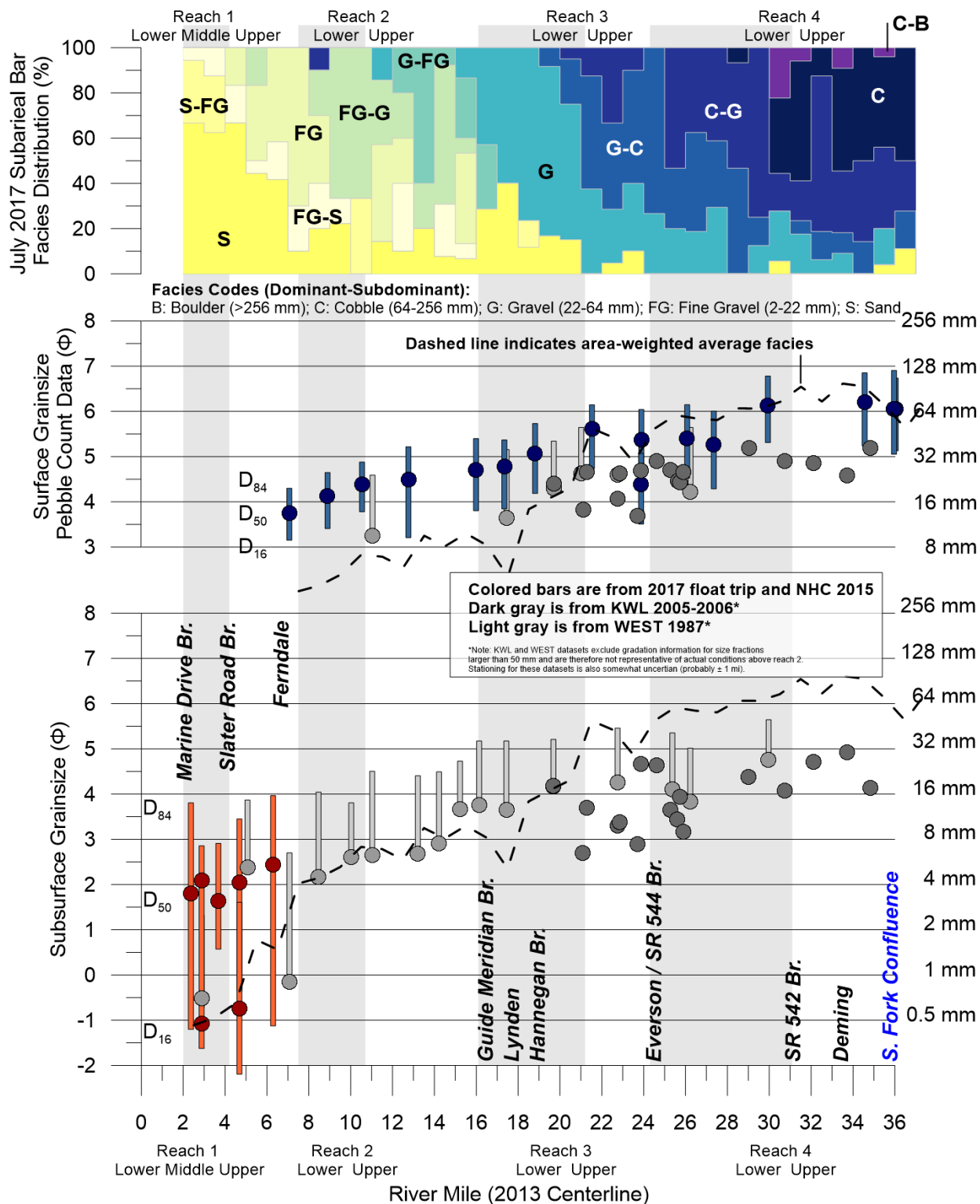


Figure 15: Summary of bed material grainsize data along the Nooksack River.

The final zone of declining grainsize begins at the upstream edge of Lower Reach 2 and extends down to the gravel-to sand transition at about RM 5. The lowest bar coarse enough for a pebble count was at RM 6.4. Between RM 9.9 and the bar at RM 6.4, D_{84} and D_{50} values decline from 29 to 20 mm and from 21 to 13 mm, respectively ($\alpha_{d50} = 0.06$ and $\alpha_{d84} = 0.1$). Fine gravel remains abundant on the bed down to just below Slater Road at about RM 4, and below that sand becomes nearly ubiquitous with few patches of fine gravel (see NHC, 2015 for a detailed description of this area).

3.2.2 Bank Material and Vegetation Stabilization of Eroding Banks

Field observation confirms the general applicability of KWL’s model of bed and bank material composition for Upper Reach 3 through Reach 4, but shows conditions are very different in Lower Reach 3 and downstream (an area that was not the focus of KWL’s work). A layer of sand or sand and silt, the depth of which depends mostly on the age of the floodplain surface and history of overbank sedimentation, consistently overlies a gravel or cobble and gravel fill deposited to about the typical height of bars through the reach (Photo 1). Where present, the sand unit in this area gradually increases in thickness from about 2 ± 0.8 feet in Upper Reach 4 to 4 ± 3 feet in Upper Reach 3. The thickness of the gravel unit depends mostly on the local depth of scour along the eroding bank and increases with distance downstream from Upper Reach 4 through Upper Reach 3 from a characteristic eroding thickness of about 8 feet to about 12 feet downstream (Figure 16).

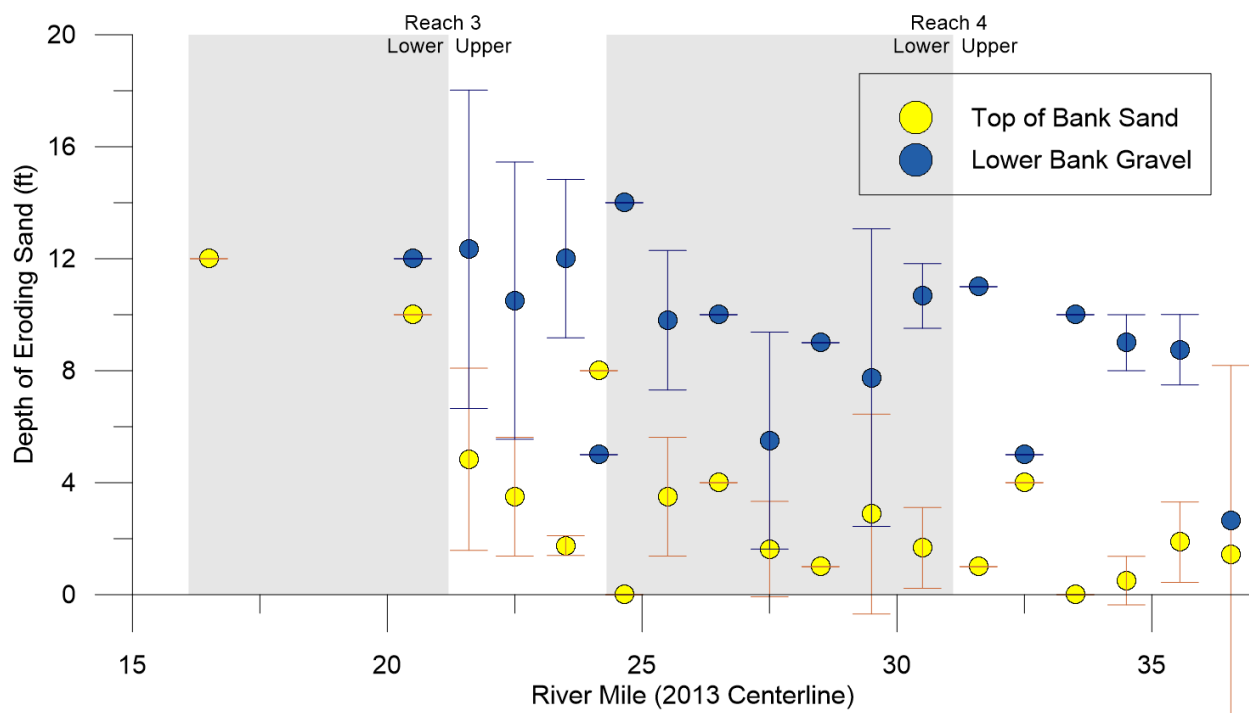


Figure 16: Thickness of upper bank sand or silty sand and lower bank gravel or cobble-gravel bank stratigraphic units.

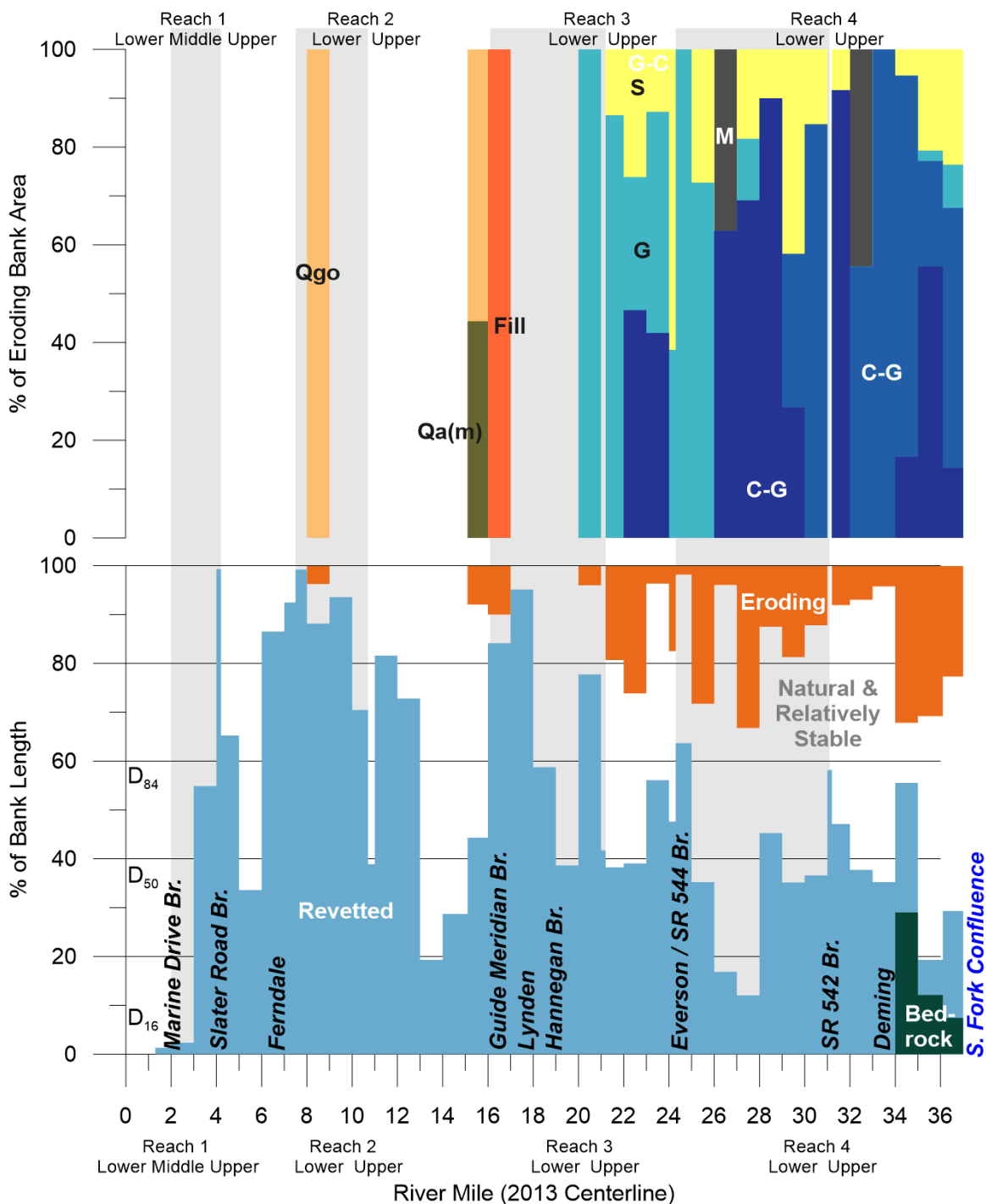


Figure 17: Observed pattern of bank conditions (bottom) and facies distribution in eroding banks (top). Facies codes are the same as in Figure 15 with additional values M — Silt, Fill, Qa(m)—Quaternary alluvium consisting of silt, clay, and abundant organic material and wood believed to have been deposited in a lacustrine or low-energy floodplain environment, and Qgo—recessional glacial outwash.



Photo 1: A characteristic example of cutbacks in Reach 4 showing floodplain sand overlying gravel. Also note the limited stabilization from the roots of this immature cottonwood stand.

The character of eroding banks changes dramatically from the upstream to downstream side of Lower Reach 3. Major bank erosion is relatively restricted, but observed exposed banks from the downstream side of Lower Reach 3 through Lower Reach 2 consistently contain material that is not Nooksack River alluvium (Figure 17). This includes recessional glacial outwash —unit Qgo— in channel fills (Photo 2) that cut through and underlie consolidated and cohesive muddy sediment — unit Qa(m)— (Photo 3) interpreted to have been deposited in a lacustrine, floodplain, or possibly shallow marine environment. The material in both of these units would be expected to have higher bank strength than the alluvial gravels exposed from Upper Reach 4 through Upper Reach 3, but the cohesive clayey material likely has substantially higher bank strength than the recessional outwash —this may explain the pattern of observed bank erosion tending to correspond to areas of the bank where the outwash is locally exposed.

The roots of vegetation provide additional stability to channel banks, particularly where they are composed of unconsolidated sediment. Figure 18 shows how the depth of bank stabilized by vegetation roots increases with the age of the trees present along the bank. Notably, however, late seral mature Mixed Riparian Forest (Photo 4) appears to have a lower depth of root stabilization than mature Cottonwood dominated forest (Figure 18). Mature willow was never associated with eroding banks, but was present through Reach 2 and locally elsewhere. It forms very dense root mats to below the low-flow water surface. Appendix C maps the condition of riparian forest in detail, and so details of the observed forest along eroding banks are not described here.

Bank material and cohesion provided by roots of riparian vegetation are a key parameter controlling bank erosion rates and channel cross-section geometry. Presence of cohesive bank material and deep rooted riparian vegetation in Reach 1 through Lower Reach 3 is conducive to lower migration rates and a narrower, deeper channel than upstream where low bank strength tends to allow more rapid bank erosion and promote a wide, braided channel planform. The magnitude of these influences is quantified relative to hydraulic and bed material forcing in Section 5.



Photo 2: Example of recessional glacial outwash exposed in a Nooksack River Cutbank.



Photo 3: Fine consolidated grained silt and clay with abundant wood and organic material characteristic of banks through Reach 2 and potentially Lower Reach 3.



Photo 4: Moderately deep root stabilization provided by Mature Mixed Riparian Forest.

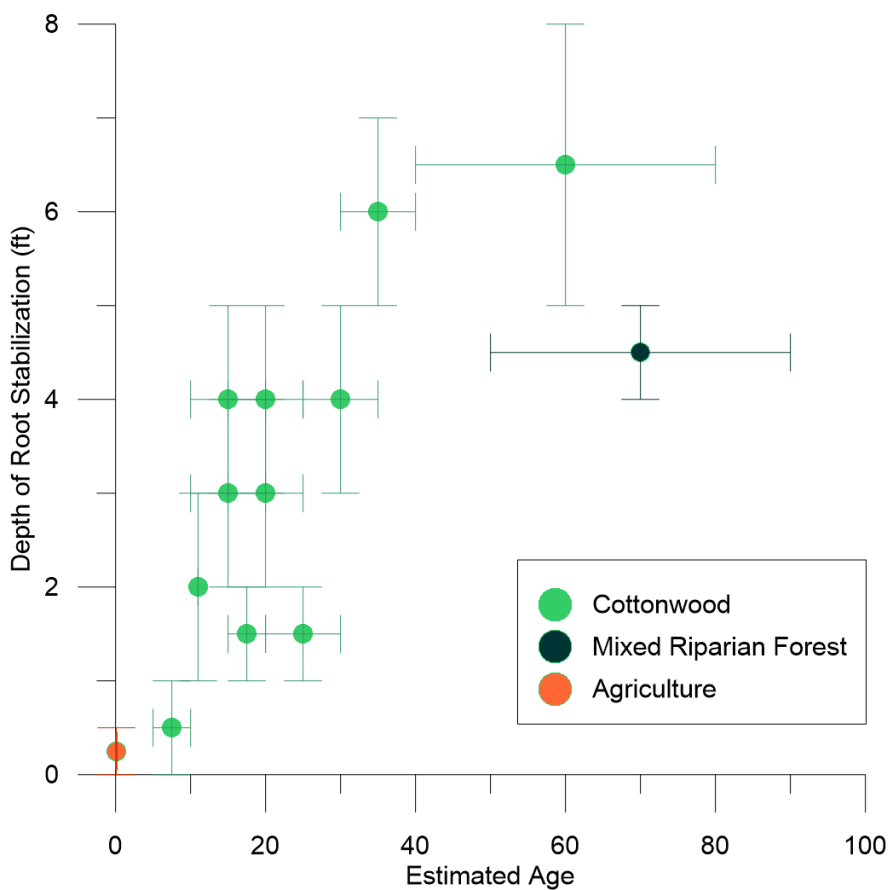


Figure 18: Depth of observed root stabilization by age of bank top vegetation.

4 SEDIMENT MOBILITY PATTERN

Comparing the hydraulic and grainsize distribution data described above with each other elucidates along-channel sediment transport and connectivity patterns. Figure 19 shows observed grainsize data, thalweg shear stress profiles, and bed material normalized shear stress computed for several flood-maximum water surface profiles.

The normalized shear stress $\left(\frac{\tau^*}{\tau_c^*}\right)$ is a measure of the excess shear stress available to transport sediment. It is the ratio of the Shields stress (τ^* , sometimes denoted as θ) to the critical dimensionless shear stress required to mobilize the bed material τ_c^* , assumed in these calculations to be 0.03. Shields stress is computed as follows:

$$\tau^* = \frac{\tau}{(S - 1) \rho g D}$$

where τ is the bed shear stress (in this case computed from the FEQ output using the depth-slope product), S is the specific density of the sediment (here assumed to be a typical value of 2.65), ρ is the density of water (1000 kg/m³), g is acceleration due to gravity, and D is the grainsize of interest expressed in m. Values of $\frac{\tau^*}{\tau_c^*}$ greater than 1 indicate sediment mobility while values less than 1 indicate the bed is mostly stable. For simplicity, Figure 19 has assumed a typically used constant value of τ_c^* , even though this value varies substantially when the bed consists of a mixture of sizes depending on the ratio of the subject grainsize to that of the surrounding material. The value used in these calculations was 0.03, which is appropriate for coarser material in a gravel-bed river, but values ranging from as high as 0.055 (van Rijn, 1984) to as low as 0.02 are plausible (e.g. Andrews, 1983) —particularly for the coarsest grains on the bed. Using a value of 0.02 would increase the $\frac{\tau^*}{\tau_c^*}$ value by a factor of 0.5.

The Rouse number (P) provides another parameter for understanding sediment transport. It is given by the following relation:

$$P = \frac{w_s}{K u_*}$$

where w_s is the sediment settling velocity, K is the von Karman constant (0.4) and u_* is the shear velocity of the fluid, calculated as $u_* = \sqrt{\frac{\tau}{\rho}}$. Values greater than 2.5 indicate bedload transport, between 1.2 and 2.5 mixed suspended and bedload transport, between 0.8 and 1.2 suspended transport, and <0.8 movement as wash load. P was evaluated for coarse (1 mm), medium (0.5 mm), and fine sand (0.25 mm) and coarse silt (0.063 mm). Based on these calculations:

- fine sand and smaller material moves as wash load through the whole Lower Nooksack
- medium sand moves as wash load through Reach 4, suspended load through Upper Reach 2, and both in suspension and on the bed downstream of that, and
- coarse sand moves as mixed load along the whole Lower Nooksack, except through the shear stress minima in Lower Reach 2 and Upper Reach 1.

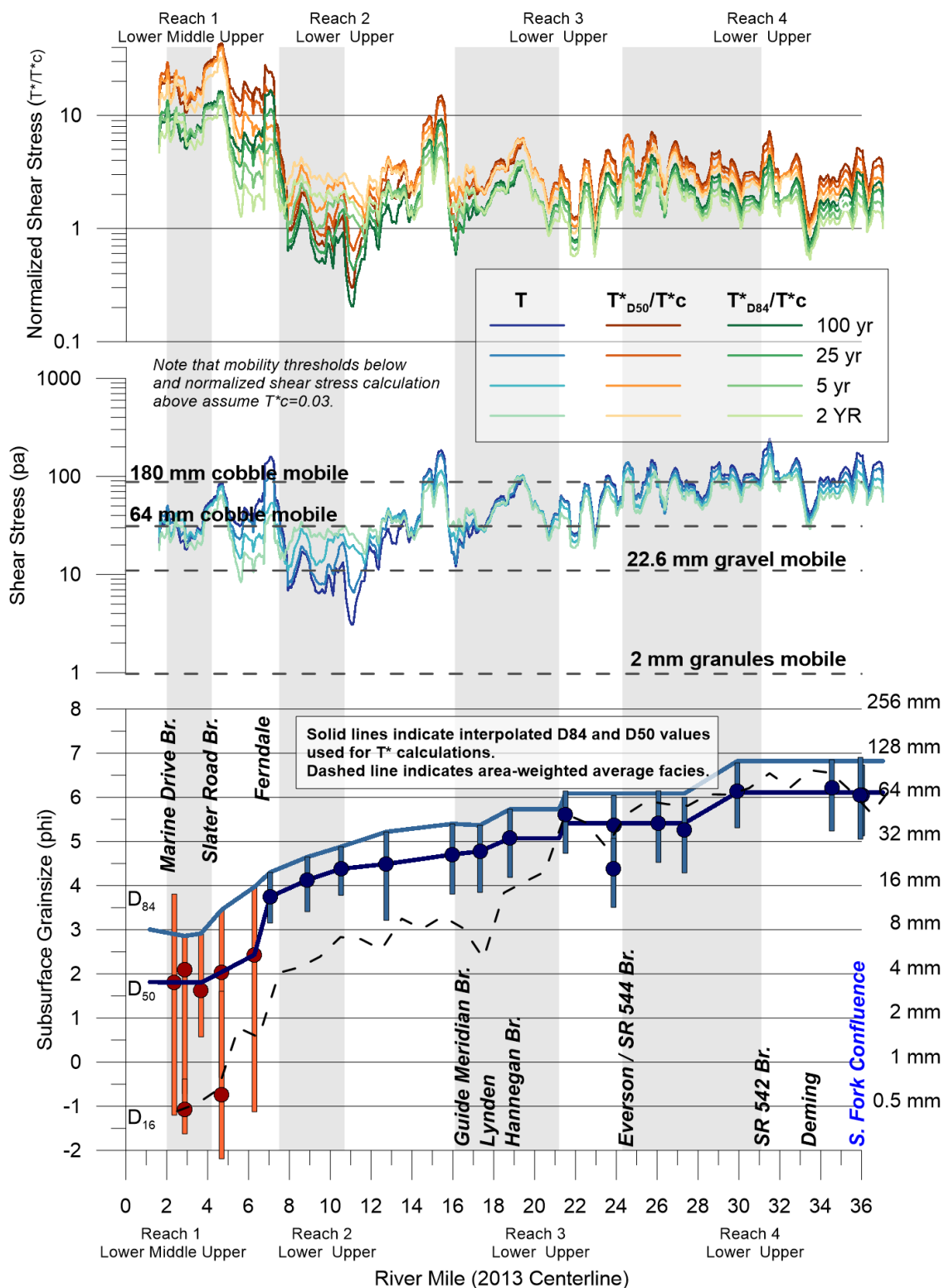


Figure 19: Comparison of channel hydraulics with bed material grainsize illustrating along-channel variability in sediment mobility. Pebble counts in blue, bulk samples in orange. (2015 and 2017 data only)

Several important patterns in sediment mobility along the river are illustrated in Figure 19. First, there is little change in shear stress from the upstream to the downstream boundaries of Reach 4, which is somewhat surprising given the notable decrease in grain size that occurs through Lower Reach 4. It is important to note that shear stress is somewhat underestimated through Upper Reach 4 because the depth used in the calculation is from the flood water surface to the low-flow water surface and not thalweg. Taken together the relatively constant shear stress and downstream reduction in bed material grain size would suggest increasing sediment transport competence through Lower Reach 4. There is no indication from sediment transport mobility calculations that the constriction above—and into—the Everson Bridge forms a significant blockage to the downstream conveyance of bed material.

In contrast, sediment mobility plummets from upstream to downstream through Upper Reach 3, with $\frac{\tau^*}{\tau_c^*}$ dropping from 1 to 6 through Lower Reach 4 to reach values of 0.7 to 2 toward the downstream edge of Upper Reach 3. Maximum calculated flood $\frac{\tau^*}{\tau_c^*}$ values at local minima near the boundary between Upper and Lower Reach 3 are about 1, indicating that this is an area of substantial competence limitation controlling downstream sediment conveyance. This observation, combined with the declining normalized shear stress trend across Upper Reach 3, suggests that this is likely an area of active and substantial net movement of coarse sediment into long-term storage.

Normalized shear stress increases and then decreases to reach another local minima from upstream to downstream across both Lower Reach 3 and Upper Reach 2, particularly during larger floods when backwater effects of prominent constrictions just below the Guide Meridian Bridge at Lynden create substantial ponded backwater regions upstream. These sequences are forced by “floodplain flow cells”, where tight constrictions forcing all flow through a narrow corridor around the main channel alternate with areas where flow—up to about 2/3 of the total discharge during the 100-yr event—can flow through the large flood basins along the valley margins. In the constrictions, the water surface slope is relatively steep, flow deep, and shear stress correspondingly high. Sediment supplied to these areas from upstream is relatively fine-grained compared to the locally severe hydraulic conditions and, therefore, readily flushed through as indicated by the high normalized shear stress. During larger flood flows, water that had escaped into the floodplain returns to the channel above the next constriction downstream and forms a backwater along the channel upstream; this shear stress reversal probably limits sediment conveyance during larger events and may lead to aggradation during extreme floods—followed by later evacuation. During the 2-yr flow, the shear stress minima at the bottom of Lower Reach 3 is higher than the minima upstream, and so downstream sediment transport rates are still likely regulated by export from Upper Reach 3.

The shear stress minima in the downstream portion of Upper Reach 2 extends through Lower Reach 2 to the constriction formed by a combination of Pleistocene sediment and bridge abutments at Ferndale. This area has an extreme shear stress reversal where increasing flow produces decreasing shear stress and, therefore, sediment mobility for all flows above the 2-year recurrence interval flood. The highest shear stress in this area likely occurs during a flow substantially lower than the 2-year peak. Physical evidence—that is a general lack of bars and gently concave channel profile—does not suggest substantial sediment accumulation in this reach and so these lower flows are interpreted to have the capacity to ultimately convey the material that accumulates during floods.

From Upper Reach 1 through Middle Reach 1, sediment mobility increases as the bed material shifts from gravel- to sand dominated conditions. This is largely a result of the low-tide downstream simulation boundary condition, but the calculated shear stress shows competence to move gravel all the way into Lower Reach 1. NHC (2015) interpreted the shift from gravel to sand to occur mostly in response to sand dropping out of suspension onto the bed and diluting gravel transport, as opposed to a competence limitation for downstream movement of fine gravel.

5 REGIME AND PLANFORM GEOMETRY

Rational Regime Theory provides a useful tool for examining the key factors controlling the channel planform and hydraulic geometry, and potential flexibility in the channel form due to natural variability in water and sediment supply and anthropogenic changes—including both historic and potential future management actions. It is a robust physically-based approach to predicting channel dimensions that has been validated against a large empirical dataset. The UBC regime model (UBCRM Eaton et al., 2004; Eaton, 2007; Millar et al., 2014) is based on this approach and accounts for many more of the key controlling variables than traditional empirical regime equations while maintaining limited enough required input data to be readily applicable. The model utilizes the controlling variables shown in Table 2, which importantly include specification of a bank strength parameter (μ). This parameter is defined as the ratio of the critical shear stress required to mobilize the bank material to the critical shear stress required to mobilize the bed sediment. Bank strength integrates effects of the grain size distribution, cohesion, and influence of vegetation roots, which increase the tensile strength of the bank soil.

Only one of the input parameters is not quantitatively known through the study area. Channel forming flow (Q , here taken as the 2-yr main channel discharge in groups varied stepwise down the river at major breaks), reach slope (S), and the bed material grain size distribution (D_{50} and D_{84}) are well known; while the default value of τ^* was retained. The value of μ is not quantitatively known, but the general observations of bank characteristics suggest it is typically near unity through Reach 4, likely relatively high in Reaches 1 through Lower Reach 3, and transitional through Upper Reach 3. The model was calibrated to existing conditions by entering the known input parameters (listed in Table 2) and varying μ until the approximate observed active channel width was reproduced. This calibration procedure is a recommended approach (Eaton, 2015; personal communication) to evaluating conditions utilizing the model.

Results of the regime analysis are summarized in Figure 20, which plots expected channel dimensions and bedload transport rate during the channel forming flow against varied bank strength and channel forming flow. Human activities have had the potential to change bank strength by modification of riparian vegetation (typically decreasing bank strength) and construction of revetments (increasing bank strength) and to change Q_{cf} by modifying flow patterns through the construction of levees, bridges, and other flow control features.

Table 2: Calibrated parameterization for UBCRM Calculations

Input Parameter	Upper Reach 4	Lower Reach 4b	Lower Reach 4c	Upper Reach 3	Lower Reach 3	Upper Reach 2	Lower Reach 2	Upper Reach 1
Q (cfs)	33,500	33,500	32,000	32,000	32,000	26,500	22,000	22,000
S (ft/ft)	0.002	0.002	0.0025	0.00175	0.0004	0.0005	0.0003	0.0003
D₅₀ (mm)	66	70	42	41	49	26	21	13
D₈₄ (mm)	120	110	71	66	71	42	29	20
τ^*	0.02	0.02	0.02	0.02	0.02	0.02	0.02	0.02
μ	1.01	1.01	1.05	1.5	1.25	1.5	2	1.5

5.1 Bank Strength

Channel cross-section sensitivity to bank strength is explored in the left “column” of Figure 20, where bank strength is varied across the X-axis and channel forming flow held constant. These results indicate that bank strength is extremely low (near unity) in Reach 4 and moderate (1.5 to 2) in Reach 1 through Reach 3. In other river systems, channels with continuous revetments typically have substantially higher bank strength values (3 to 4); the comparatively low bank strength interpreted for Reach 1 through Lower Reach 3 (1.25 to 2) suggests relatively limited reach-scale influence of revetments in controlling the average channel cross-section from Reaches 1 through Lower Reach 3. Furthermore, the channel cross-sectional form in Reach 2 and Lower Reach 3 is very insensitive to the bank strength but appears to be controlled by variability in the channel forming flow and slope. The biggest anthropogenic impacts on the channel morphology in Reaches 1 through Lower Reach 3 are interpreted to result from changes in the channel length due to meander cutoffs and changes in partitioning of channel-forming flood flow between the channel and valley bottom.

The natural bank strength of Upper Reach 3 may be transitional between the channel downstream and Reach 4 and the relatively high bank strength in Upper Reach 3 (as compared to Reach 4) may suggest a relatively strong geomorphic influence of revetments along this segment of the river.

Very low existing bank strength through Reach 4, correspondingly, means that this portion of the river would be expected to be relatively sensitive to bank hardening, an inference that is supported by the relatively significant local changes in the channel cross-sectional form where it is entrained against hard banks through this reach.

There is one additional notable implication of the interpreted bank strength relative to the channel width. The maximum predicted channel width for Upper Reach 4 and Lower Reach 4B are 700 and 900 feet, respectively, similar to the present channel but much narrower than the historic channel belt width. Even with a substantial increase in Q_{cf} , these historic channel widths are not reached. This result highlights the important role that island-forming stable large wood jams played as a governing control on the channel morphology in this area. The historic channel belt width included large stable vegetated islands and many anabranching channels where flow was forced to spread through a much broader corridor than would apparently have occurred in the absence of stable large wood.

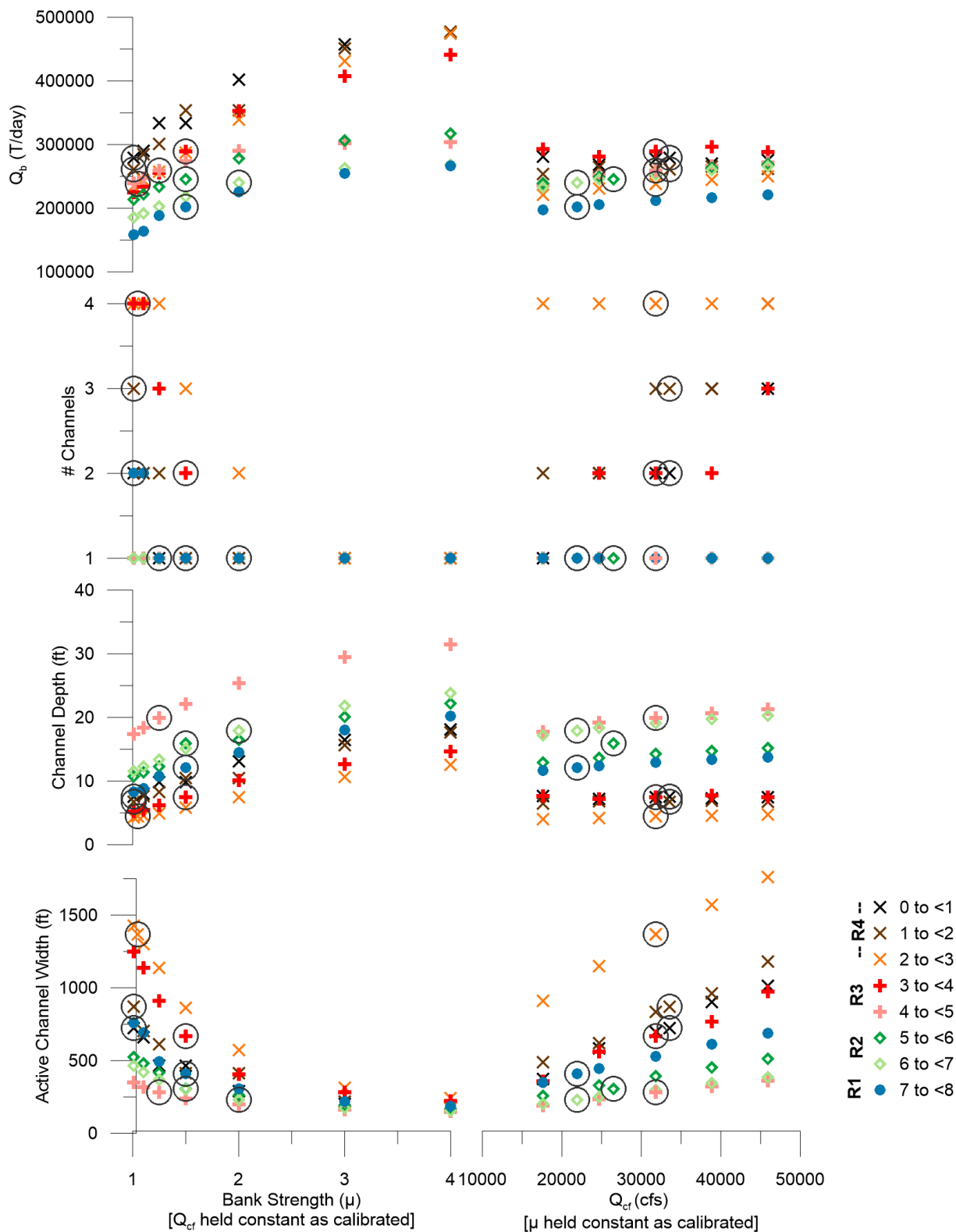


Figure 20: Summary of UBCRM calculations illustrating channel sensitivity to varying bank strength and channel forming flow. Table 2 lists calibrated values of μ and Q_{cf} . Circled values represent calibrated condition.

5.2 Channel Forming Discharge

Floodplain storage and conveyance through floodplain flow paths result in a substantial reduction in the peak discharge for the 2-year flow in downstream reaches, with even more substantial impacts at higher flows (Figure 2 and Figure 3), especially as flow begins to spill out of the basin towards Sumas.

Construction of levees and other flow modification features may have impacts on the channel forming flow through the study area, with the biggest potential impacts in Reach 1 through Lower Reach 3. In addition, natural climate variability and anthropogenic climate change may both impact the magnitude of the channel forming flow, and so sensitivity to channel forming flow is also illustrated in Figure 20. The right “column” of plots holds bank strength constant and varies channel forming flow. As with bank strength, Reach 4 is the most sensitive to changes in the channel forming discharge. This is followed by Upper Reach 3 and then by Reach 1.

5.3 Slope

The regime analysis indicates that Reach 2 and Lower Reach 3 are remarkably insensitive to changes in bank strength and channel forming discharge. Another important anthropogenic modification has occurred with the highest intensity in this area: channel straightening, which has reduced the sinuosity and therefore increased the slope. The potential impact of this modification was evaluated by estimating the historic slope for these reaches based on the change in sinuosity and running the regime model for the calibrated existing condition but modifying the slope. Table 3 summarizes these results and suggests that only Reach 3 would be predicted to have responded in a measurable way to the change in slope, with the channel presently wider than it would be at its lower historic slope. The mean channel belt width has actually declined through Reach 3 relative to the historic condition (see accompanying main report), another indication that the planform of this reach has been particularly impacted by bank hardening revetments.

Table 3: Summary of estimated changes in channel slope and corresponding change in width.

	Proportion change in sinuosity	Estimated historic slope	Width with historic slope (ft)	Current width (ft)	Proportion change in width
Upper Reach 3	-0.21	0.0014	482	667	-0.38
Lower Reach 3	-0.25	0.00032	255	281	-0.10
Upper Reach 2	-0.14	0.00044	319	307	0.04
Lower Reach 2	0.08	0.00033	238	232	0.02

6 KEY LARGE-SCALE PROCESSES CONTROLS GOVERNING CHANNEL MORPHODYNAMICS

River processes through the Lower Nooksack River are organized by the large-scale controlling template resulting from the legacy of the Late-Holocene channel avulsion from a course north to the Canadian border at Sumas into its present alignment downstream to Bellingham Bay. Dynamic adjustment to the avulsion appears to be ongoing along the river profile. The most acute impact occurs in the areas closest to the avulsion node: a signal of degradation and bed material coarsening appears to be propagating upstream near the transition between Upper Reach 4 and Lower Reach 4; downstream of the node, gravel-cobble sedimentation is focused through Upper Reach 3 as the channel traverses across an alluvial fan-like landform formed by the alluvium deposited into the low gradient valley downstream of the avulsion.

The impact is not limited to the area proximal to the avulsion node. Channel migration through Lower Reach 3 and Reach 2 has not yet occurred to the extent needed to surround the channel with alluvium comparable to the bed material, with legacy cohesive sediment and relatively consolidated recessional outwash banks contributing to the narrow channel planform through these reaches. The impact of limited channel migration on the channel hydraulics is most acute during large floods, when constriction from Pleistocene deposits at Ferndale—enhanced by piers and abutments of co-located bridges—dramatically backs up flow above Ferndale.

Regime analysis suggests that there is limited potential to change the channel hydraulic geometry in Reach 2 and Lower Reach 3, but that Upper Reach 3 and Reach 4 are quite sensitive to change—for better or worse— in response to future channel management actions.

REFERENCES

- Anderson, S. W., and Grossman, E. E. (2015). *Topographic and bathymetric data on the mainstem Nooksack River, Fall 2015*. [online] Available from: <https://doi.org/10.5066/F72B8W7M>.
- Andrews, E. D. (1983). Entrainment of gravel from naturally sorted riverbed material. *Geological Society of America Bulletin*, 94(10), 1225–1231. doi:10.1130/0016-7606(1983)94<1225:EOGFNS>2.0.CO;2.
- Eaton, B. (2007). *The University of British Columbia Regime Model (UBCRM)- User's manual: Draft*. University of British Columbia. Vancouver, BC pp.
- Eaton, B. C., Church, M., and Millar, R. G. (2004). Rational regime model of alluvial channel morphology and response. *Earth Surface Processes and Landforms*, 29(4), 511–529.
- KWL (2005). *Nooksack River Sediment Management Plan Summary of Background Information Appendix C: Summary of Nooksack River Bed Material Samples*. Report prepared by Kerr Wood & Leidal Associates for Whatcom County Flood Control Zone District.

- KWL (2008). *Updated Sediment Analysis for Lower Nooksack River (2039.008)*. Report prepared by Kerr Wood & Leidal Associates for Whatcom County Flood Control Zone District. [online] Available from: <http://www.co.whatcom.wa.us/publicworks/riverflood/pdf/sediment-analysis.pdf>.
- Linsley, Kraeger Associates, Ltd. (2004). *Lower Nooksack River Unsteady-Flow Model and Analysis of Initial Scenarios Near Everson, Whatcom County, Washington*.
- Millar, R., Eaton, B., and Church, M. (2014). *UBC Regime Model*. [online] Available from: <http://ibis.geog.ubc.ca/~beaton/UBC%20Regime%20Model.html> (Accessed 19 March 2015).
- NHC (2015). Appendix C: Geomorphic Characterization. *Lower Nooksack River Project: Alternatives Analysis*. Report prepared by The Watershed Company, LandC, Etc., Northwest Hydraulic Consultants, and Cardno for Whatcom County.
- Rice, S. (1999). The nature and controls on downstream fining within sedimentary links. *Journal of Sedimentary Research*, 69(1).
- van Rijn, L. C. (1984). Sediment transport, part I: bed load transport. *Journal of hydraulic engineering*, 110(10), 1431–1456.
- Wentworth, C. K. (1922). A scale of grade and class terms for clastic sediments. *The Journal of Geology*, 30(5), 377–392.
- Wolman, M. G. (1954). A method of sampling coarse river-bed materials. *Transactions of the American Geophysical Union*, 35(6), 951–956.

NHC Ref. No. 2002455

February 11, 2019

Applied Geomorphology Inc.
211 N. Grand Suite C
Bozeman, MT 59715**Attention:** **Karin Boyd**
Principal Geomorphologist**Via email:** kboyd@appliedgeomorph.com**Re: Nooksack River Geomorphic Assessment: Detailed Upper Reach 3 Regime Analysis**

Dear Ms. Boyd:

NHC is assisting Applied Geomorphology with the Lower Nooksack River Geomorphic Investigation for Whatcom County. As a part of our work in this project, we completed a rational regime assessment of conditions along the river. This assessment is reported in Section 5 of NHC's primary project report, which is included as Appendix C for the main project report. That documentation summarizes the model used and general methodology. You have requested that NHC explore potential controls on the historical transition of Upper Reach 3 from a meandering to braided planform, with particular attention to whether historical changes in the reach's slope, which increased following meander cutoffs and a reduction in sinuosity, may explain the planform transition. Channel pattern and slope are characteristically related, with an increasing tendency towards braiding at steeper slopes for a given bed material grainsize distribution and hydrology (Church, 2006). This relationship has been documented in various channel pattern discrimination plots and functions (e.g. Leopold and Wolman, 1957), but a regime model formulation allows an greater number of potentially controlling variables to be considered (Eaton et al., 2010).

The UBC Regime Model (UBCRM) was used to evaluate to this hypothesis. The model is described in Appendix C and documentation by its authors (Eaton et al., 2004; Eaton, 2007; Eaton and Church, 2007; Eaton et al., 2010). In the model I reduced the reach slope from 0.00175, the present condition, to 0.00144 simulating a an increase in sinuosity from the current value of 1.1 to the historic value of 1.4 to represent a best estimate of the historic conditions. I kept the other input parameters as calibrated to the existing condition (Table 2 in appendix C). Initial results are described in Section 5.3 of appendix C, which show the reduced slope would be expected to narrow the channel significantly but both slopes have two channels. However, this threshold is extremely close; additional testing showed that it occurs at a slope of 0.00140, only an additional 3% reduction, which is very much within the uncertainty for the

historic reach slope. Applying only the sinuosity increase probably underestimates the actual historic slope for the reach because I expect there has been preferential aggradation at the upstream side of Upper Reach 3 compared to the downstream side, which would also have increased the slope of the reach.

Because of the inherent uncertainty in estimating historic conditions for the reach, I applied formal uncertainty and sensitivity analyses to the historical slope condition. For the uncertainty analysis a Monte Carlo analysis was performed, sampling 1,600 permutations of the input parameter set from the defined plausible range. For this assessment, input parameter variability was assigned to represent a moderate level of uncertainty: from the best estimate of the historic conditions described above flow was given a ± 20 percent range, slope a ± 10 percent range, D_{50} a ± 20 percent range, D_{84} a ± 20 percent range, and μ a ± 20 percent range. From the upstream channel base case, flow was given a ± 30 percent range, slope a ± 90 percent range, D_{50} a ± 45 percent range, D_{84} a ± 5 percent range, and μ a ± 50 percent range.

Results of the uncertainty analysis (Figure 1) support the hypothesis that the slope change could easily have caused the reach to cross a transition from a single thread sinuous planform to a braided planform: 45% of cases resulted in a single thread, 43% in two channels, and the remainder three or more channels.

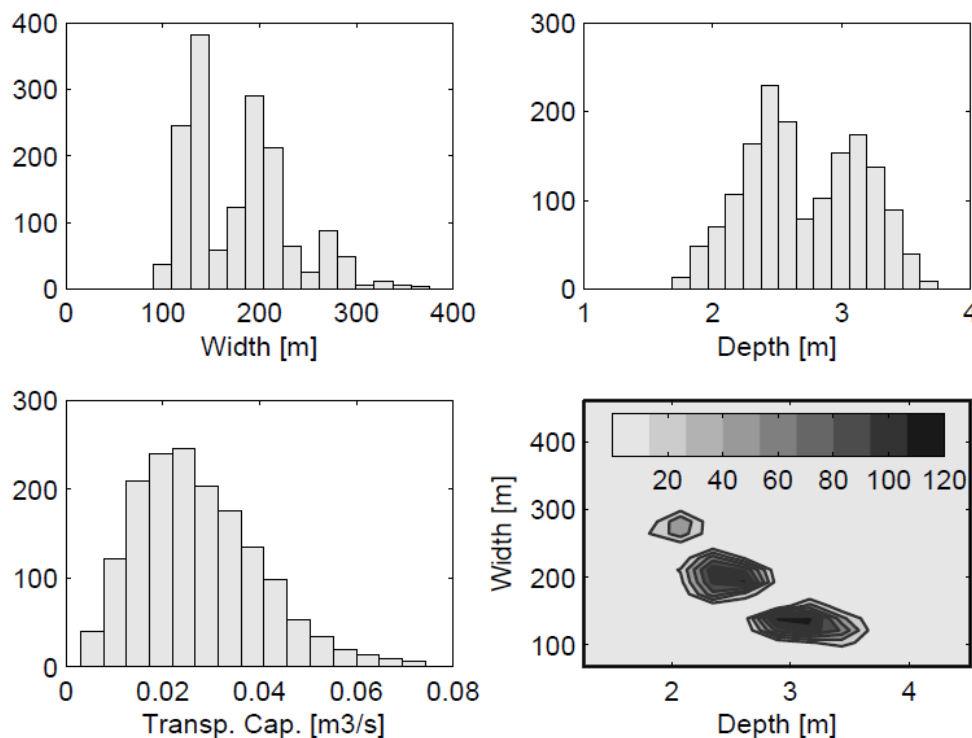


Figure 1: UBCRM sensitivity analysis with Monte Carlo sampling of input parameters.

Note values shown are in metric units and scale of the axes are different between panels.

The sensitivity analysis systematically varied one input parameter and held all others constant to show which controls have the biggest impact on the resulting channel form. For this assessment, the best estimate of historic conditions described above was varied over a ± 20 percent sensitivity range (Figure 2). In the figure, model-output width, depth, and transport capacity are normalized to the base case and plotted on the dimensionless y-axis, while the ± 20 percent perturbation in each input parameter is shown on each dimensionless x-axis.

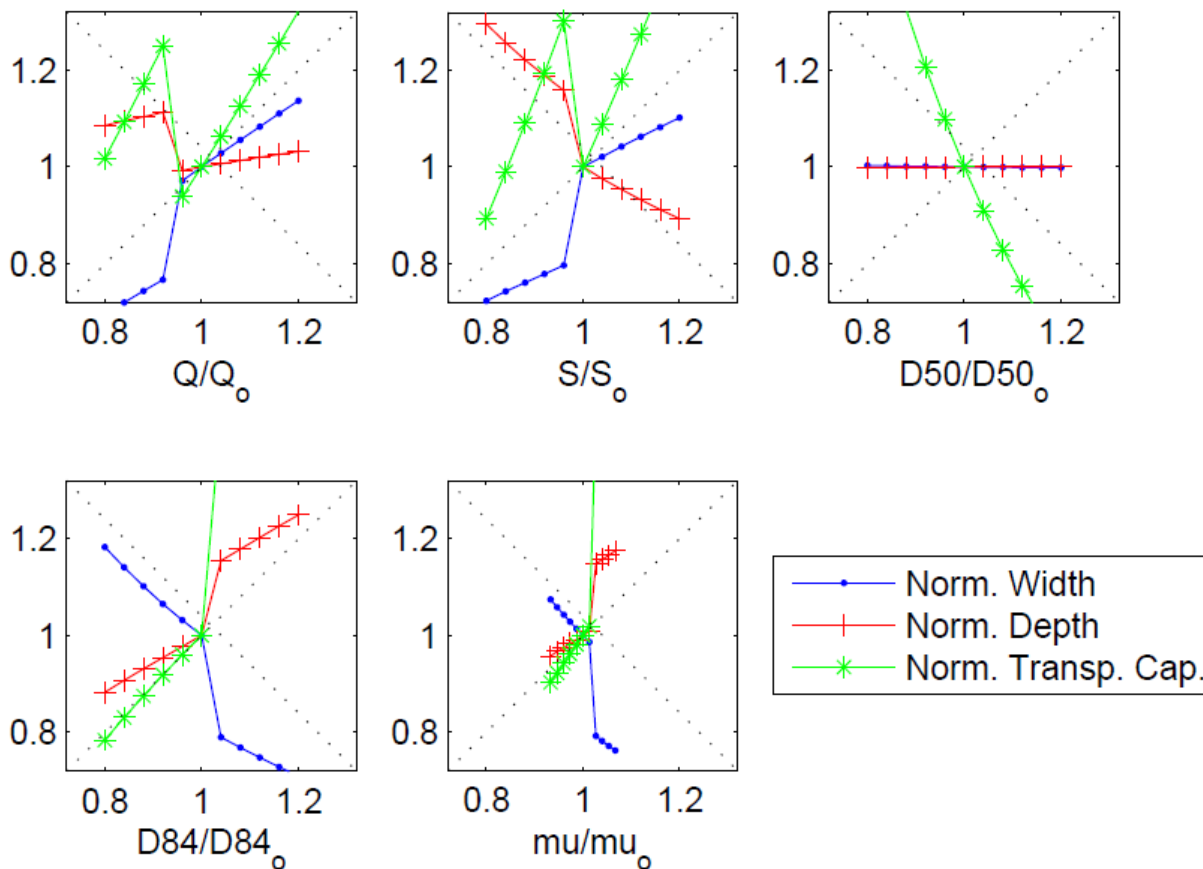


Figure 2: UBCRM sensitivity analysis with systematically varied individual boundary conditions (note μ represents bank strength). The Y axes for all plots represent the values for width, depth, and transport capacity normalized to the base-case value. For instance, a value of 1.2 for any given parameter would mean that it is 20% greater than for the base case. Interestingly, at the transition from two channels to a single thread with reduced discharge (Q) and slope (S), channel width decreases and depth increases disproportionately to the reduction in energy from lower Q or S . This results in an initial increase in the transport capacity.

These results show that the channel width which, other parameters being equal directly controls the planform (Eaton et al., 2010) is extremely sensitive. Small reductions in any of slope, Q , $D84$ or increase in bank strength (μ) result in a rapid reduction in width and transition to single thread condition. This

finding, combined with the results of the uncertainty analysis strongly suggests the following two principal conclusions:

- A) The reach was historically very close to a transition from single to multi-thread planform.
- B) The best estimate of the slope change is just barely not sufficient to force the planform change. It may be that the real slope change was slightly greater or that a change in one or more additional factors also influenced the change.

DISCLAIMER

This document has been prepared by Northwest Hydraulic Consultants Inc. in accordance with generally accepted engineering practices and is intended for the exclusive use and benefit of Applied Geomorphology and Whatcom County and their authorized representatives for specific application to the Nooksack River near Everson, WA, USA. The contents of this document are not to be relied upon or used, in whole or in part, by or for the benefit of others without specific written authorization from Northwest Hydraulic Consultants Inc. No other warranty, expressed or implied, is made. Northwest Hydraulic Consultants Inc. and its officers, directors, employees, and agents assume no responsibility for the reliance upon this document or any of its contents by any parties other than Applied Geomorphology and Whatcom County.

Sincerely,

Northwest Hydraulic Consultants Inc.

Prepared by or under the direct supervision of:

ANDREW D. NELSON

Andrew Nelson, L.G.
Senior Geomorphologist
Analysis and Reporting

Dave McLean
Principal River Engineer
Reviewer